6

A New Look at the Hydrophobic Characteristics of Cyclodextrins and Their Inclusion Complexes

Abstract: In a brief review of the conformational properties of cyclodextrins, their torus-like shape with the secondary 2- and 3-OH groups being located on the wide opened rim and the 6-CH_2OH units canted towards the center cavity is illustrated. Color-coded visualizations of the molecular lipophilicity patterns (MLP) on the contact surfaces of α-, β-, γ-, and δ-CD unequivocally establish the hydrophobic nature of their central cavity. On the basis of these molecular modelings and some fundamental thermodynamic principles, the role of hydrophobic interactions for the formation of inclusion complexes is discussed. As exemplified for a number of inclusion complex structures it is demonstrated that in many cases the hydrophobicity patterns of the cyclodextrins determine the orientation of the guest molecule within the cavity. Most notably, the MLP's of per-*O*-methyl substituted cyclodextrins reveal their inverse type hydrophobic topographies. Future implications of these molecular modeling techniques in molecular recognition and supramolecular chemistry are outlined.

Cyclodextrins, small cyclic maltooligosaccharides with six (α-CD) to nine (δ-CD) glucose residues, are accessible from enzymatic degradation of starch[304]. These naturally occurring cyclodextrins have received considerable attention as versatile complexing agents for small organic molecules which are incorporated in the hydrophobic center cavities of the cyclodextrins[305-309].

Cyclodextrins

α (n = 1)
β (n = 2)
γ (n = 3)
δ (n = 4)

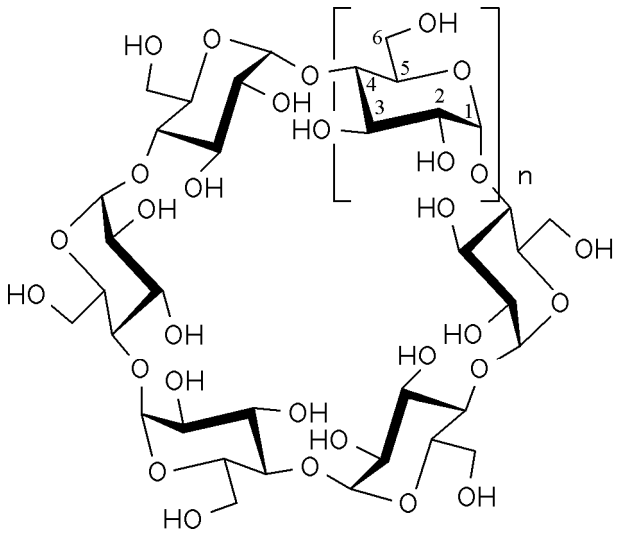

The overall hydrophilicity of the cyclodextrins makes them ideal carriers for pharmaceuticals for example, increasing the bioavailability by enhancing their water

solubility[310a-d]. Cyclodextrins also serve as protectants for encapsulated compounds which are volatile or sensitive to air, heat, light, and / or hydrolysis[310b,e]. Scarcely any other class of organic compounds comprises a so multifarious range of practical applications in pharmaceutics, chromatography[310f,311], diagnostics[310g], environmental biotechnology[310h,i], industrial applications[312] and processes such as the selective removal of cholesterol from egg yolk[313] for example, and even catalysis[314,315].

Basically all industrial purposes for which the cyclodextrins are used[316] are related to their ability to form stable, non-covalent inclusion complexes of well-defined stoichiometry with entirely different guest compounds. Many of these interesting cyclodextrin complexes were characterized not only by NMR methods[317], but also by solid state X-ray or neutron diffraction structural analysis[318,319]. However, so far, the hydrophobic component of the guest-host interactions in molecular recognition and self-assembly leading to the formation of the inclusion complexes has been studied by augmentation of simple molecular models only. Molecular modeling techniques now provide more sophisticated tools for the assessment of relevant hydrophobic effects. In this chapter, a systematic and comparative reappraisal of the pivotal hydrophobic characteristics of the native cyclodextrins should be given. Prior to this, some special features of their conformational properties obtained from statistical analysis of solid state structures are outlined, inasmuch as they are relevant to the evaluation and discussion of their **m**olecular **l**ipophilicity **p**atterns (**MLP**'s).

Molecular Geometry of Cyclodextrins

Statistical analysis of solid state geometries of all cyclodextrins contained in the Cambridge Crystallographic data file (CCDF)[192] (for details see Appendix I) was performed to obtain the mean molecular geometry parameters for α-, β-, and γ-cyclodextrins. The recent X-ray structure of the δ-CD hydrate[320] was also included, but since the coordinates neither were deposited in the CCDF file, nor were they provided by the authors[320] upon request, a special procedure was employed to reproduce the three-dimensional structure from the molecular plot given in the short communication of the structure determination (see Appendix II).

The global molecular shape of cyclodextrins can be described by basic molecular parameters, such as torsion angles, interatomic distances, and virtual bond lengths (see Fig. 6-1). The relevant mean structural descriptors for the cyclodextrins are listed in Table 6-1.

In each class of cyclodextrins, the glucose units adopt a rather stiff[318] $^4C_1$-conformation, with little divergences of the mean ring torsion angles

Θ_1 (C_2-C_3-C_4-C_5) and Θ_2 (C_3-C_4-C_5-O_5) from ideal undistorted values (cf. Table 6-1). Deviations of these dihedral angles from the equilibrium values become important in the calculated structures of the synthetic lower ring homologs of the natural cyclodextrins only (this work, Chapter 8). By considering the heavy atoms C-1 to C-6 and O-1 to O-5 (but not O-6) least-squares fitting of all glucose units via rigid body rotation[128] showed root-mean-square (RMS) fluctuations of the atomic positions of 0.07(4) Å only. In addition, the Cremer-Pople (CP) ring puckering parameters[122,124] for the monosaccharide units – in particular the puckering angle θ of approximately 0 to 10° – are consistent with this finding of uniform glucose $^4C_1$-shapes[321].

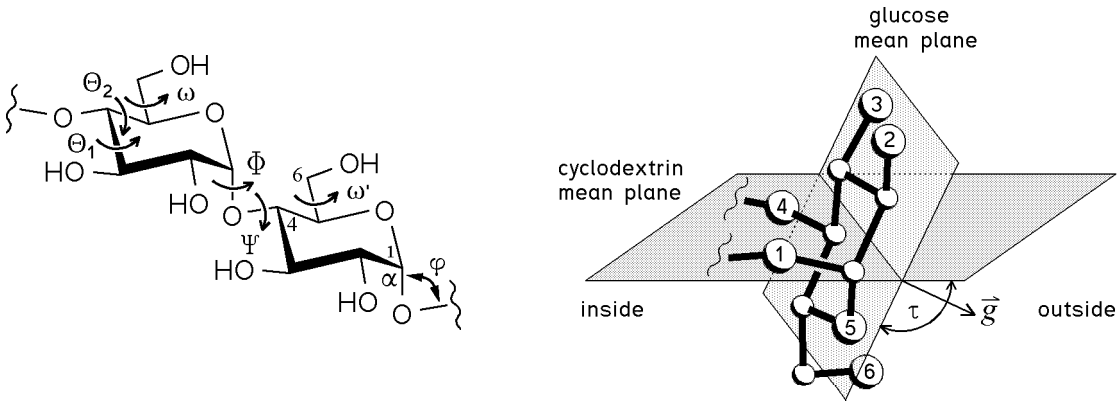

Fig. 6-1. Cyclodextrin geometry descriptors: the intersaccharidic bond angle φ is defined by the atoms C_1-O_1-$C_{4'}$, the torsion angles which describe the conformations about the glycosidic linkages are denoted Φ (O_5-C_1-O_1-$C_{4'}$) and Ψ (C_1-O_1-$C_{4'}$-$C_{3'}$). The endocyclic ring torsions around C-4 are named Θ_1 (C_2-C_3-C_4-C_5) and Θ_2 (C_3-C_4-C_5-O_5), the exocyclic torsion angle ω (O_5-C_5-C_6-O_6) describes the orientation of the primary 6-OH relative to the pyranoid ring, whereby the three staggered conformations are referred to as *gauche-gauche* (*gg*, $\omega \approx -60°$), *gauche-trans* (*gt*, $\omega \approx +60°$), and *trans-gauche* (*tg*, $\omega \approx \pm 180°$). The tilt angle τ denotes the inclination of the pyranose rings towards the macrocyclic ring perimeter, i.e. the angle between the cyclodextrin mean plane of all oxygens involved in the intersaccharidic linkages (the anomeric O-1) versus the least-squares best-fit mean plane through the six pyranoid ring atoms (C_1-C_2-C_3-C_4-C_5-O_5 with the normal vector *g*, *right* plot; hydrogen atoms were omitted for clarity). Absolute values of $|\tau| > 90°$ indicate the 6-CH_2OH side to be turned towards the center cavity. A positive sign of τ correlates with the upper face (clockwise view on $C_1 - C_5$ and O_5) of the sugar moieties (and the vector *g*) pointing towards the outside of the macrocyclic ring*.

* The tilt angle τ was preferred over the alternative angle τ' (cf. Ref. [319]) between the cyclodextrin mean plane and the best-fit plane of O_1, C_1, C_4, and O_4 of each glucose residue, since τ directly correlates with the almost perpendicular orientation of the glucose units in regard to the cyclodextrin macro ring system, yet $\tau \approx \tau' + 90°$.

Table 6-1. Cyclodextrin mean molecular parameters obtained from statistical crystal structure analysis for α-, β-, γ-, and δ-cyclodextrin geometries[319] (root-mean-square (RMS) deviations in parenthesis).

CD n		structures[a] N_1 / N_2	torsion angles[b] $<\Theta_1>$	$<\Theta_2>$	Cremer-Pople parameters $<Q>$	$<\theta>$	$<\phi>$[c]	glucose conformation
6	α	46 / 54	52.3(5.1)	-53.0(6.2)	0.577(0.036)	5.7(4.8)	120.2	$^4C_1$
7	β	44 / 50	55.1(5.9)	-55.8(4.8)	0.579(0.037)	5.2(5.2)	170.5	$^4C_1$
8	γ	9 / 24	61.7(6.0)	-62.2(5.8)	0.613(0.053)	8.4(4.3)	234.4	$^4C_1$
9	δ	1 / 1[d]	53.3	-57.5	0.566	3.6	323.6	$^4C_1$

CD n		torsion angles[a] $<\Phi>$	$<\Psi>$	angle[e] $<\varphi>$	tilt[f] $<\tau>$	distances [Å] $<O_1\text{-}O_{1n'}>$[g]	$<O_2\text{-}O_{3'}>$	$<C_6\text{-}C_{6'}>$
6	α	107.4(6.6)	130.7(8.5)	118.2(2.1)	102.1(7.1)	8.51(0.23)	3.05(0.55)	4.45(0.21)
7	β	110.5(7.6)	127. (11.)	117.6(2.7)	100. (10.)	9.81(0.31)	2.92(0.27)	4.59(0.22)
8	γ	110.1(4.0)	129.4(4.1)	115.0(3.0)	104.4(2.8)	11.76(0.07)	2.84(0.06)	4.39(0.13)
9	δ	112. (16.)	122. (19.)	118.9(8.0)	105. (23.)	12.46(1.23)	3.01(0.19)	4.66(0.50)

a) A total of N_1 different solid state structures with N_2 crystallographically independent molecules were analyzed. – b) Φ: $O_5\text{-}C_1\text{-}O_1\text{-}C_{4'}$, Ψ: $C_1\text{-}O_1\text{-}C_{4'}\text{-}C_{3'}$, Θ_1: $C_2\text{-}C_3\text{-}C_4\text{-}C_5$, Θ_2: $C_3\text{-}C_4\text{-}C_5\text{-}O_5$. – c) for $\theta \rightarrow 0°$, the puckering angle φ and the corresponding RMS deviations become meaningless, since $^4C_1$-conformations are identical to $^2C_5$ and $^OC_3$. – d) due to the mode of generation of the single δ-CD structure (see text) the RMS fluctuations of some molecular parameters are irrelevant. – e) φ: $C_1\text{-}O_1\text{-}C_{4'}$. – f) angle between best-fit mean plane of the macro ring (defined by all O_{1n}-atoms) and each glucose-mean plane (atoms C_1 to C_5 and O_5). – g) $O_1\text{-}O_{1n}$-distances (in Å) diagonal across the cyclodextrin ring.

The structure of the cyclodextrins is determined by the cyclic α(1→4)-type linkages, with all secondary 2-OH and 3-OH groups being located on one side of the torus shaped molecule, whilst the 6-CH_2OH groups make up the opposite rim. Out of the three staggered conformers of the hydroxymethyl groupings only two are populated to a significant extent, since in the solid state as well as in solutions the *gt* rotamer of the *gluco*-series is generally disfavored by 1,3-diaxial-like repulsions between O-4 and O-6[53,67-73]. In methyl α-D-glucoside the *gg* ($\omega \approx -60°$) and *gt* rotamers ($\omega \approx +60°$) are almost equally important[73], whereas in the solid state structures of cyclodextrins an approximate ratio of *gg* : *gt* ≈ 3.5 : 1 is found (Fig. 6-2). Unless intermolecular hydrogen bonding with a guest molecule included in the center cavity of the cyclodextrins can take place the *gg* conformer with the 6-CH_2OH-groups pointing towards the outside of the ring is favored.

The intersaccharidic bond angle φ ($C_1\text{-}O_1\text{-}C_{4'}$) as well as the torsion angles Φ ($O_5\text{-}C_1\text{-}O_1\text{-}C_{4'}$) and Ψ ($C_1\text{-}O_1\text{-}C_{4'}\text{-}C_{3'}$) observed in the solid state structures of α- to δ-cyclodextrins (Table 6-1) do not vary to a large extent (Fig. 6-2), no significant

changes with increase of the ring size could be deduced. The Φ / Ψ-torsions agree with measurements of the ^{13}C-^{1}H-NMR coupling constants for α- to γ-CD peracetates, which allow a direct assessment of the alternative intersaccharidic torsions Φ' (H_1-C_1-O_1-$C_{4'}$) and Ψ' (C_1-O_1-$C_{4'}$-$H_{4'}$) via a Karplus-type relationship[324]. Most notably, the mean values of Φ and Φ' are approx. 20 – 30° smaller than Ψ and Ψ' (Φ ≈ Φ' + 120° and Ψ ≈ Ψ' + 120°), respectively.

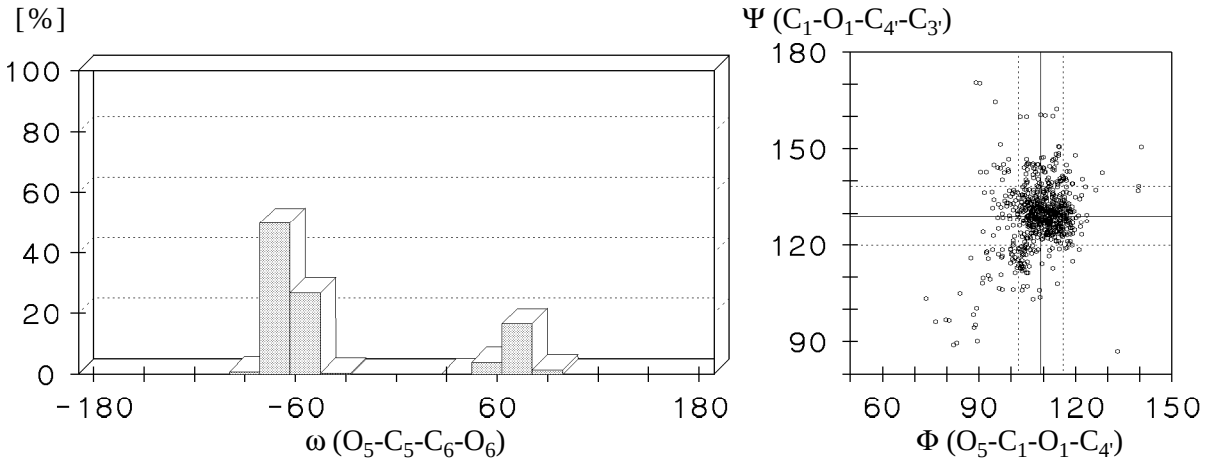

Fig. 6-2. Probability distribution of the hydroxymethyl conformations (ω torsion angle, *left* plot) and scatter plot of the intersaccharidic Φ / Ψ-torsion angles (*right* side) derived from α-, β-, γ-, and δ-cyclodextrin solid state geometries (altogether 129 crystallographically independent molecules in 100 different structures). In addition, the mean values and the respective RMS deviations of the Φ / Ψ-angles are marked by solid and dotted lines.

The Φ / Ψ-torsions correlate with the relative orientation of the glucose residues in respect to the macrocyclic ring. The glucose tilt angles τ (Fig. 6-1) are considered to be even more depictive, since they directly illustrate the canting of the monosaccharidic units. The mean values around 100 – 105° found for the tilt angles τ in all cyclodextrin classes are synonymous with a rotation of the primary 6-hydroxyl groups towards the center cavity of the torus. In consequence, the opposite molecular side made up by the secondary 2- and 3-OH groups represents the wider opened torus rim.

The width of the probability distribution of the τ-angle (Fig. 6-3) and the respective RMS-fluctuations (Table 6-1) indicate a certain degree of conformational flexibility inherent in the cyclodextrins. As evident, the glucose units invariably prefer inclination such that the 6-CH_2OH groups point towards the molecular center (τ > 90°). As indicated by the low distribution width, the γ-cyclodextrins seem to prefer higher symmetry conformations with limited flexibility of the intersaccharidic linkages only. However, the opposite holds true for the δ-CD: the widespread distribution of the

glucose inclinations in the single solid state structure indicates that steric strains, which are introduced by increasing the cyclodextrin ring size, can be diminished by asymmetric deformation of whole macrocycle. Simultaneously, the conformational space accessible to the glucose moieties by rotation around the intersaccharidic linkages and the overall molecular flexibility increases.

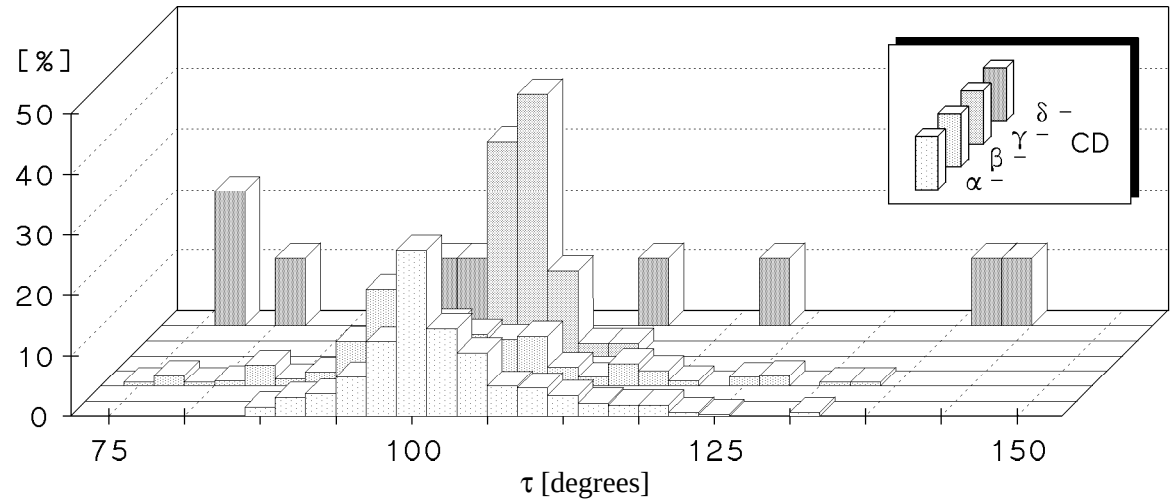

Fig. 6-3. Probability distribution of glucose tilt angles τ observed in the crystal structures of α-, β-, γ-, and δ-cyclodextrins.

Analogous trends could be observed for the O_1-$O_{1n'}$-distances diagonal across the cyclodextrin rings. Beside the increasing ring diameter, the corresponding distribution plots (Fig. 6-4, upper plot) indicate the conformational flexibility of α- and β-cyclodextrins. Their molecular shapes can adapt to different sizes of included guest molecules by asymmetric distortion. The very narrow probability distribution found for γ-CD geometries again illustrates their symmetric structures, while the δ-CD is distorted to a significant extent. Furthermore, the internal RMS-deviations of the O_1-$O_{1n'}$-distance parameters within the various cyclodextrins (Fig. 6-4, lower entry) are consistent with these findings. Due to the high symmetry a small range of variations is observed for the γ-cyclodextrins, while the high RMS fluctuation in δ-CD again reflects the large elliptical distortion of this structure.

Referring back to a the work of van Helden *et al.*[325], the extent of elliptical distortions of the cyclodextrin macrocyclic ring can also be described by a distortion parameter, defined as the ratio of the minimal and maximal O_1-$O_{1n'}$-distance of each cyclodextrin structure[326]. The observed values (Fig. 6-5) around 0.99 for γ-cyclodextrins again illustrate their symmetrically round-opened structures, while the extent of distortion is largest for the δ-CD ($d_{min}/d_{max} \approx 0.76$).

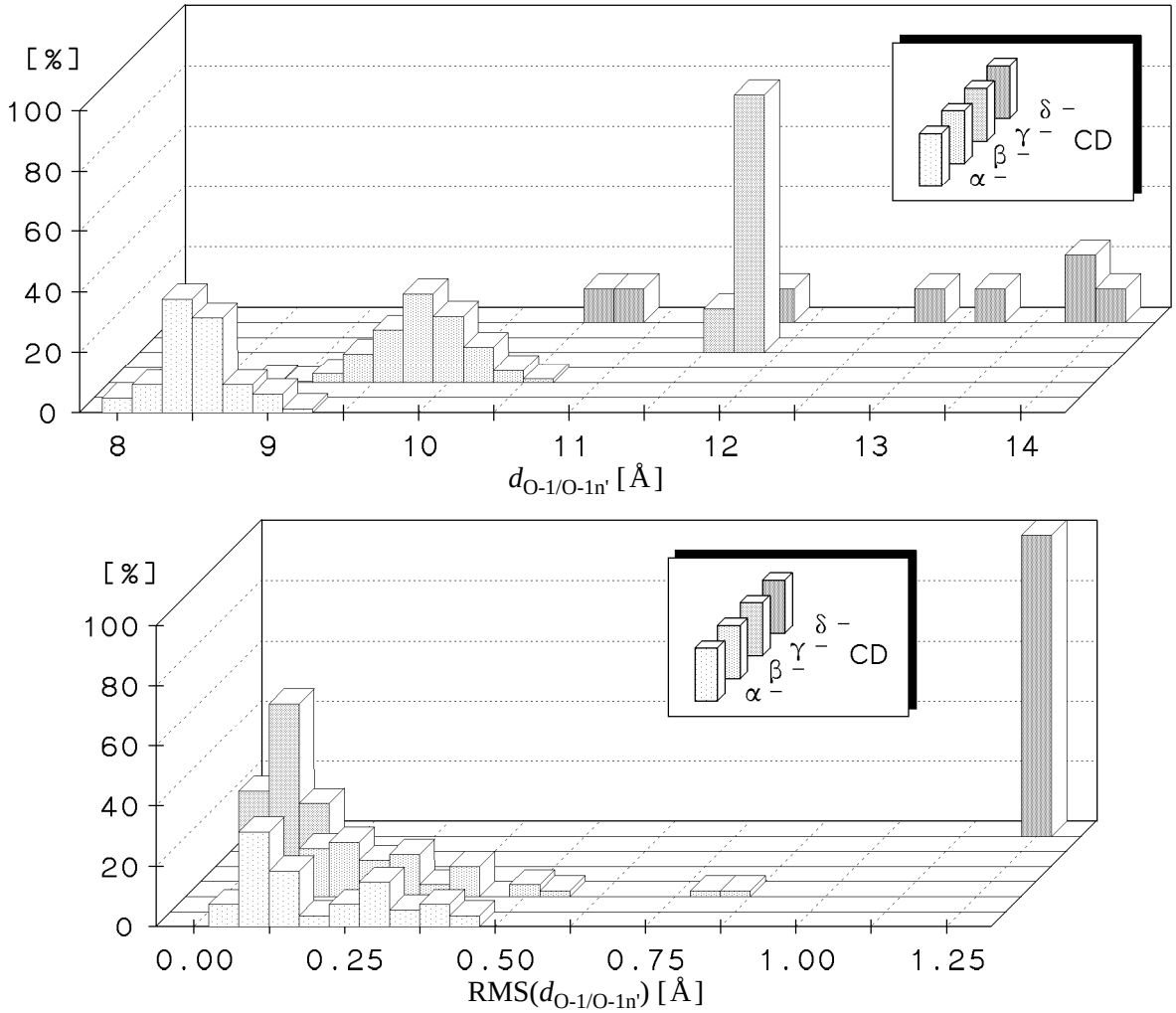

Fig. 6-4. Percentage distribution of O_1-$O_{1n'}$-distances diagonal across the macrocyclic ring (in Å) in relation to the cyclodextrin ring size (crystal structural data, *upper* diagram). The *lower* plot illustrates the range of the RMS-fluctuations of the O_1-$O_{1n'}$-distances observed in each cyclodextrin structure, low fluctuations indicate symmetric structures, high values correspond to elliptical distortions.

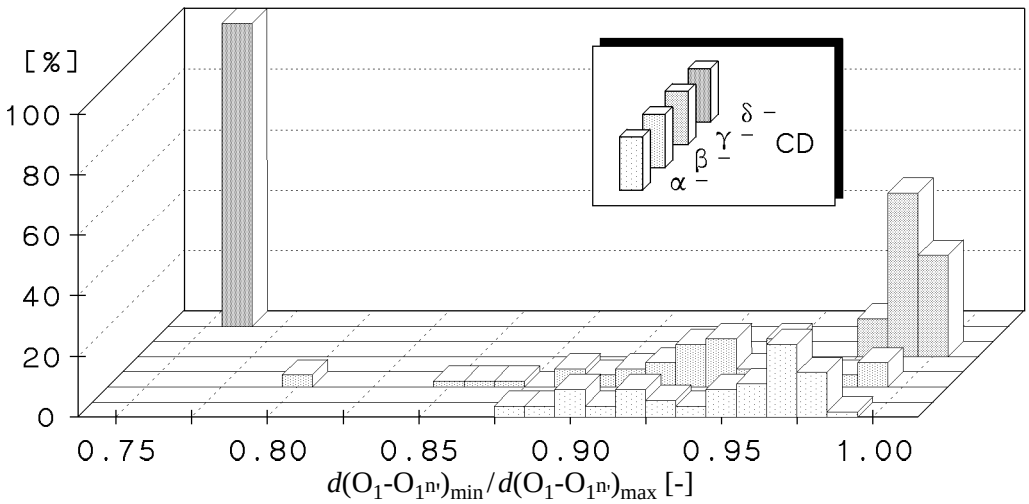

Fig. 6-5. Probability distribution of the cyclodextrin distortion parameter, i.e. the ratio of the minimal and maximal O_1-$O_{1n'}$-distances across the macrocyclic ring, as derived from the crystal structures of α-, β-, γ-, and δ-cyclodextrins.

Characteristic for cyclodextrins are the low O_2-$O_{3'}$-distances[318,327,328] (cf. Table 6-1) between adjacent glucose units, which decrease from 3.06(55) Å in α-cyclodextrins, to 2.92(27) Å in β-cyclodextrins and 2.84(6) Å in γ-cyclodextrins (recalc. values). The opposite increase of the mean distance in δ-CD is caused by growing distortion and bending of the macrocycle itself. Obviously, the close contact between O-2 and O-3' is stabilized by interresidue hydrogen bonding between both hydroxyl groups, a type of intramolecular interaction which is not only limited to the solid state structures of cyclodextrins[318,327,328], but was also established by IR-experiments to prevail in solution[329]. Thereby, the decreasing distances account for the larger conformational flexibility of α-CD in relation to its larger homologs β- and γ-CD[306]. The favorable hydrogen bonding interaction not only decreases the chemical reactivity of the 3-OH group dramatically[329], it is also responsible for the considerably enhanced reactivity of the 2-OH groups – in particular when compared to the primary 6-OH – in the course of the sodium hydride induced alkylation of the cyclodextrins[330], for example. The alkoxide anions primarily formed under these conditions are most effectively stabilized by intramolecular hydrogen bonding between the neighbored O-2 and O-3' oxygen atoms[139,140], leading to a concentration of the main charge density at O-2. In consequence, the ensuing trapping reaction of the anions with alkylating agents is characterized by a high regioselectivity in favor of the glucose 2-position[330].

The large C_6-$C_{6'}$-distances of approximately 4.4 – 4.7 Å (Table 6-1) and the rotational flexibility of the primary hydroxyl groups – in particular when bearing in mind that the C_6-O_6-bonds preferentially point away from the center of the molecule – disfavor the formation of an analogous interresidue hydrogen bonding network at the opposite side of the cyclodextrin torus.

The multitude of solid state structures displays a considerable degree of conformational flexibility inherent in the various cyclodextrins[319,327]. In agreement with force field based computational studies, these compounds represent by no means rigid truncated cone structures[331,332]. In addition, it has been noted that symmetry breaking of cyclodextrins may lower their potential energy substantially[332]. However, on the basis of the crystal structure data set it can be concluded that the overall puckering of the macrocyclic rings is generally small. This is evidenced by the low mean absolute values of the virtual torsion angles formed by four consecutive O_1-ring atoms ($|\theta_{O\text{-}O}|$) of less than 6° (α-CD: 5.1°, β-CD: 5.8°, and γ-CD: 2.3°) as well as by the average root-mean-square (RMS) deviation of the O_1-atoms from planarity (i.e. compared to the least-squares best-fit mean plane defined by all O_1-atoms) of only 0.1 Å (α-CD: 0.08 Å, β-CD: 0.12 Å, and γ-CD: 0.02 Å). Low puckering distortions of the macroring perimeter are typical for cyclodextrins[318,319]. Similar results were

obtained from a detailed high temperature annealing (HTA) study of the α-CD structure by using the CHARMM force field (Chapter 8).

Albeit cyclodextrins exhibit a certain degree of flexibility, it should be noted that its extent obviously has been overestimated in a previous MM2 and AMBER molecular mechanics (MM) analysis[332]. Despite the fact, that no statements concerning the mode of structure generation have been made, nor has the nature of the energy minima been explored thoroughly, asymmetric and highly distorted cyclodextrin conformations were proposed as global energy minimum structures[332]. In addition, too large values were computed for the $\theta_{O\text{-}O}$ torsion angles when comparing the data with the parameters obtained from solid state structures, e.g. large values of $|\theta_{O\text{-}O}| \approx 33°$ were calculated for α-CD, while the maximum torsion found in the crystal geometries amounts to 16.8° only.

A molecular dynamics study on α-CD unequivocally demonstrated that force field calculations on cyclodextrins for *in vacuo* conditions suffer from errors in the calculated structures which originate from an overestimation of hydrogen bonding interactions (see Chapter 8). Indeed, the basically wrong conclusion that the glucose residues are inclined with the 6-CH_2OH units away from the center of the cyclic oligosaccharides in the afore mentioned MM-study[332] originates from too high H-bond energies. The proposed contraction of the cyclodextrin torus at the side of the secondary hydroxyl groups is caused by the formation of an extensive intramolecular hydrogen bond network.

Molecular dynamics (MD)[333-335] and free energy calculations[132,336] with explicit consideration of polar solvent (e.g. water) molecules surrounding the cyclodextrin can be used to obtain more detailed insights in the time-dependent stereochemical features of these molecules and the relative stabilities of their complexes. In view of the rather high amount of computer time consumed by this type of calculations, the general properties of cyclodextrins should be discussed on the basis of crystal structure data only.

Solid State Structures of Cyclodextrin Hydrates as Models for "Empty" Solution Conformations

Non-complexed cyclodextrins can be crystallized from aqueous solutions as their hydrates containing 6 – 13% (w/w) water, all the corresponding solid state structures have been studied by X-ray and / or neutron diffraction analysis. Depending on the conditions applied for crystal growth, three different polymorphic forms have been found for the smallest natural cyclodextrin (α-CD · 6 H_2O, form I[337] and II[338], and α-CD · 7.57 H_2O, form III[339]). Both forms I and II exhibit almost identical conically

distorted conformations of the cyclodextrin unit with O_1-$O_{1n'}$-distances of 8.11 – 9.18 Å ($<d(O_1\text{-}O_{1n'})> \approx 8.6(4)$ Å) and $d_{min}/d_{max} \approx 0.88$. In the former structure, two molecules of water are included in the center cavity, whereas the latter annulus encloses one water only. In order to maximize the hydrogen bonding with water and to reduce "empty volume", one glucose unit is largely tilted towards the center of the molecule ($\tau \approx 98 - 132°$ and $<\tau> \approx 107(12)°$), such that the cavity becomes oblique and asymmetrical. The third form[339] is nearly symmetrical (O_1-$O_{1n'}$-distances of 8.15 – 8.77 Å ($<d(O_1\text{-}O_{1n'})> \approx 8.5(3)$ Å) and $d_{min}/d_{max} \approx 0.93$), albeit the somewhat larger puckering of the macrocycle itself (form I & II: mean torsion $<|\theta_{O\text{-}O}|> \approx 4.0(2.4)°$ and O_{1n}-deviations from planarity 0.07(4) Å; form III: $<|\theta_{O\text{-}O}|> \approx 8.3(5.3)°$ and $<d_{O1}> \approx 0.15(8)$ Å). Here, 2.57 water molecules are statistically distributed over four alternative positions inside the cavity. A comparative MD simulation of α-CD in the crystalline state and in aqueous solution indicated the significant inclination of one glucose residue (crystalline form I and II) to disappear upon dissolution[333,334], resulting in a conformation which certainly resembles more closely to form III than to I or II. The asymmetric overall shape of the molecule seems to be retained to at least some extent[333,334]. These results receive further support from a ^{13}C-CP-MAS-NMR-study indicating that the "partially collapsed" solid state geometry and the solution structure of α-CD differ significantly[340,341].

The main structural differences in the two β-CD clathrates β-CD · 12 H_2O[342,343] and β-CD · 11 H_2O[343,344] are found in the distribution of disordered water molecules in the host cavity. In contrast to α-CD, where partial dehydration of the crystals is accompanied by major structural changes, a solid-state ^{13}C-NMR investigation of the slow dehydration of β-CD from 12 to 10.5 H_2O indicated no loss of crystal order, nor any phase transition[345]. Both structures exhibit an almost symmetrically opened, round-shape of the cyclodextrin torus with geometry parameters $\tau \approx 84 - 114°$, $<\tau> \approx 101(9)°$, O_1-$O_{1n'}$-distances of 9.51 – 10.14 Å, $<d(O_1\text{-}O_{1n'})> \approx 9.8(2)$ Å, and $d_{min}/d_{max} \approx 0.94$; the macrocyclic perimeter is almost planar ($<|\theta_{O\text{-}O}|> \approx 7.2(3.9)°$ and $<d_{O1}> \approx 0.16(8)$ Å)). Inside the cavity, 6 – 6.5 water molecules are statistically distributed over eight crystallographic positions. Neutron diffraction analysis at room temperature and at 120 K revealed a flip-flop-type hydrogen bonding pattern with a high thermal flexibility even in the solid state[344,346]. These results received even further fortification from MD simulations of hydrated crystalline β-CD at different temperatures[334,335], no significant conformational changes where found between the crystalline state and the solution conformation[340].

For the non-complexed γ-CD hydrate several solid state structural analysis have been put forth with varying amounts of co-crystallized water (γ-CD · 17 H_2O[347], ≈ 14 H_2O[348], and 15.7 H_2O[349]), of which 5.3 up to 8.8 water molecules are included

in the cavity by random distribution over approximately twice as much different positions. The former low-temperature (120 K) structure shows significant distortions from ideal octagonal molecular symmetry[347], which are related to disordering of one glucose residue. The other geometries are almost perfectly round-shaped with slight annular distortions only[348,349], they by far represent the most symmetrical structures out of the different cyclodextrin hydrates (O_1-$O_{1n'}$-distances of 11.68 – 11.84 Å, $<d(O_1\text{-}O_{1n'})> \approx 11.75(6)$ Å, and $d_{min}/d_{max} \approx 0.99$) with little puckering of the cyclodextrin ($<|\theta_{O\text{-}O}|> \approx 6.1(3.0)°$ and $<d_{O1}> \approx 0.10(6)$ Å) and regular tilted glucose residues ($\tau \approx 89 – 113°$ and $<\tau> \approx 103(7)°$). In γ-CD · 15.7 H_2O conspicuously large values for the Cremer-Pople glucose-ring puckering angle θ[122,124] of up to 14.5° indicate relatively strong distortions of individual monosaccharide residues[349]. A recent force field based study noted the remarkably high agreement of the γ-CD · 14 H_2O structure[348b] with the fully MM2-geometry optimized conformation[350].

The only crystal structure available for δ-CD hydrate clathrate (δ-CD · 13.75 H_2O)[320] revealed an elliptically distorted molecule with a boat-type U-shape (O_1-$O_{1n'}$-distances of 10.6 – 13.9 Å ($<d(O_1\text{-}O_{1n'})> \approx 12.5(1.2)$ Å) and $d_{min}/d_{max} \approx 0.73$). Four out of the nine glucose units are canted to a large extent with the primary 6-OH groups towards the center cavity, while the others line up almost perpendicular to the cyclodextrin ring or are even inclined in the opposite direction (cf. Fig. 6-3, $\tau \approx 77 – 141°$ and $<\tau> \approx 105(23)°$). Thus, the 2,3-OH annular aperture is opened much wider than the opposite 6-CH_2OH side is. Severe puckering of the cyclodextrin ring is also indicated by the mean torsion $<|\theta_{O\text{-}O}|> \approx 26(18)°$ and O_1-fluctuations from planarity of $<d_{O1}> \approx 0.7(4)$ Å.

Solid state ^{13}C-NMR-investigations proved encapsulated water to be an essential factor determining the macrocyclic structure and to stabilize symmetrical conformations[340,351]. A comparative X-ray and neutron diffraction study on different crystal samples of perdeutero β-CD ethanol octahydrate revealed significant differences between both structures in terms of ordering and disordering of the ethanol molecule within the cavity, and the corresponding hydrogen bond networks, respectively[352]. Thus, it was concluded that slight changes in the conditions of crystal growth and / or crystal history before geometry determination result in typical fine structures (e.g. the H-bonding scheme), which are unique to each crystal of even this size only[352]. Nevertheless, in summary the heavily hydrated solid state conformations of the cyclodextrins and their complexes can be regarded as "frozen molecular images"[340,344a] for their aqueous solutions. This in particular holds true when keeping in mind that the comparative MD-analysis of the solid state and solution structures of α-CD and β-CD[333-335] indicated that the crystal structures represent a

single, but nevertheless relevant "snapshot" of the overall shape of both cyclodextrins. Even in aqueous solution the stabilization of the macrocyclic conformation by a strong interresidue hydrogen bonding network between the 2,3-hydroxyl groups[318,327,328] contributes to some rigidity of the cyclodextrins[319]. Measurements of ^{13}C-spin-lattice relaxation times in solution indeed indicated an enhanced molecular flexibility after partial destruction of this network by deprotonation[353].

As evidenced by the NMR spectra of the cyclodextrins, their time-averaged solution conformations exhibit C_n symmetry[354]. Thus, and according to the above discussion, the most symmetrical and untensed cyclodextrin hydrate structures were chosen – i.e. α-CD · 7.57 H_2O (form III)[339], β-CD · 11 H_2O[344b], γ-CD · 14 H_2O[348b], and δ-CD · 13.75 H_2O[320,355], all X-ray structures except of the β-CD, for which the neutron diffraction geometry was used – as reliable models for cyclodextrin structures in (aqueous) solution. They represent relevant starting points for a more detailed assessment of their hydrophobic topographies by molecular modeling.

The Contact Surfaces of α-, β-, γ-, and δ-Cyclodextrin

In the preceding chapters, the relevance of molecular contact (Connolly-type) surfaces[46] as estimations for solvent-accessible molecular regions[47] was outlined. In Fig. 6-6, the MOLCAD-program[48] generated surfaces for the relevant α-, β-, γ-, and δ-CD conformations are shown in dotted form. The molar volumes calculated on the basis of these surfaces correlate well with the cyclodextrin apparent molar volumes $^{\phi}V_{CD}$ obtained from density measurements of (aqueous) solutions[356] (calc. values (exp. in parenthesis), α-CD: 975(1015), β-CD: 1140(1168), γ-CD: 1305(1330), and δ-CD: 1410(–) Å^3 (≈ 160 – 165 Å^3/glucose unit each), all calc. values ± ≈ 20 Å^3). The volume of the central cavity increases from approx. 100 Å^3 in α-CD, to 160 Å^3 (β-CD), and 250 Å^3 for γ-CD*.

In particular those theoretical volume parameters indicate that the cyclodextrin pockets are filled with water molecules in aqueous solution unless other guest molecules are present. On the basis of the apparent molar volume of water ($^{\phi}V_{H2O}$ ≈ 18 cm^3/mol ≈ 30 Å^3/molecule) it can be concluded that 2 – 3 water molecules fit into the α-CD cavity, while β-CD is able to accommodate approx. 5, γ-CD even 8 – 9 water molecules. The obviously good agreement with the solid state structural data of the respective cyclodextrin hydrates (*vide supra*) indicates the usefulness of this type of surfaces to evaluate the steric features of the cyclodextrins.

* For the exact mathematical procedure applied to determine the cavity dimensions see Fig. 8-6. The U-shape conformation of the δ-CD macrocycle does not allow an unequivocal definition of the spatial boundaries of the cavity, and thus, of its volume, too.

Even more clearly, the effective molecular dimensions can be estimated from cross section cuts through the cyclodextrin torsi (cf. Fig. 6-7), the corresponding contours are shown in Fig. 6-8.

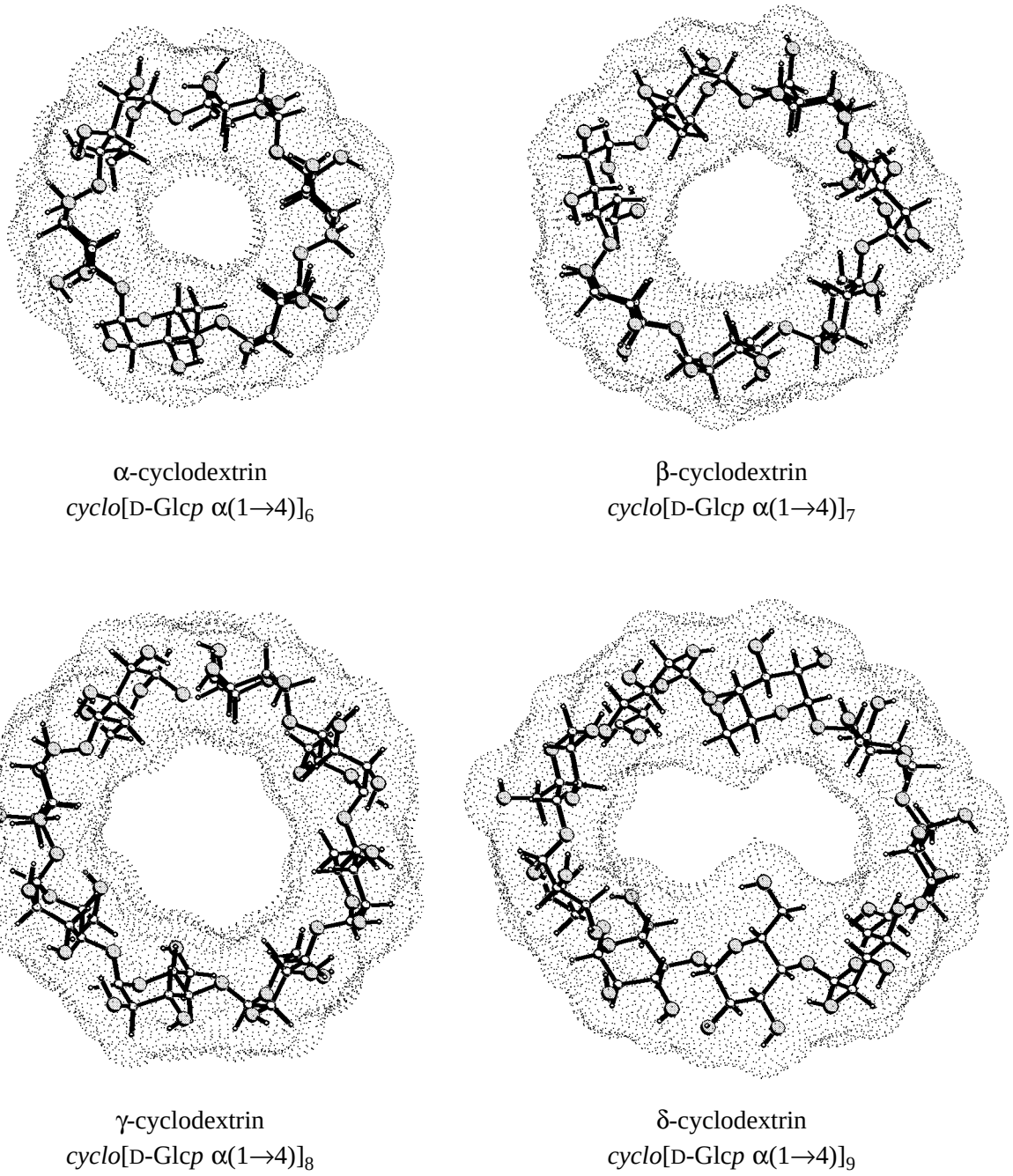

α-cyclodextrin
cyclo[D-Glc*p* α(1→4)]$_6$

β-cyclodextrin
cyclo[D-Glc*p* α(1→4)]$_7$

γ-cyclodextrin
cyclo[D-Glc*p* α(1→4)]$_8$

δ-cyclodextrin
cyclo[D-Glc*p* α(1→4)]$_9$

Fig. 6-6. Molecular geometries and dotted contact surfaces of α- (*upper left*)[339], β- (*upper right*)[344b], γ- (*lower left*)[348b], and δ-CD (*lower right*)[320,355]. The molecular orientation is uniformly such that the glucosyl 2-OH and 3-OH, i.e. the larger openings of the tori, point towards the front. The narrower openings being made up by the primary 6-OH groups are directed towards the back, respectively.

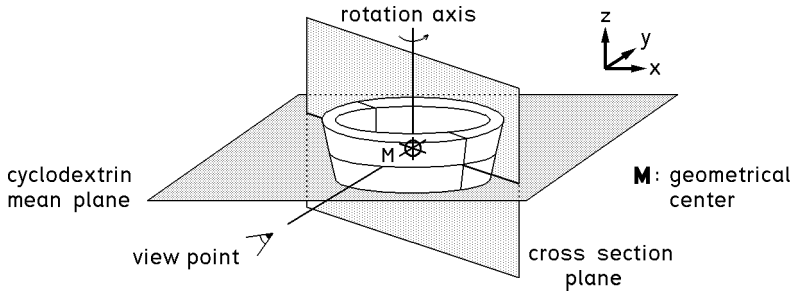

Fig. 6-7. Mode of calculation for the cyclodextrin cross section plots: surface intersections where computed with planes through the geometrical center and perpendicular to the cyclodextrin mean-plane (*x*/*y*-plane defined by all O_1-atoms) in rotation steps of 10°, and superimposed. Contours are especially suited for illustration of the effective steric molecular dimensions.

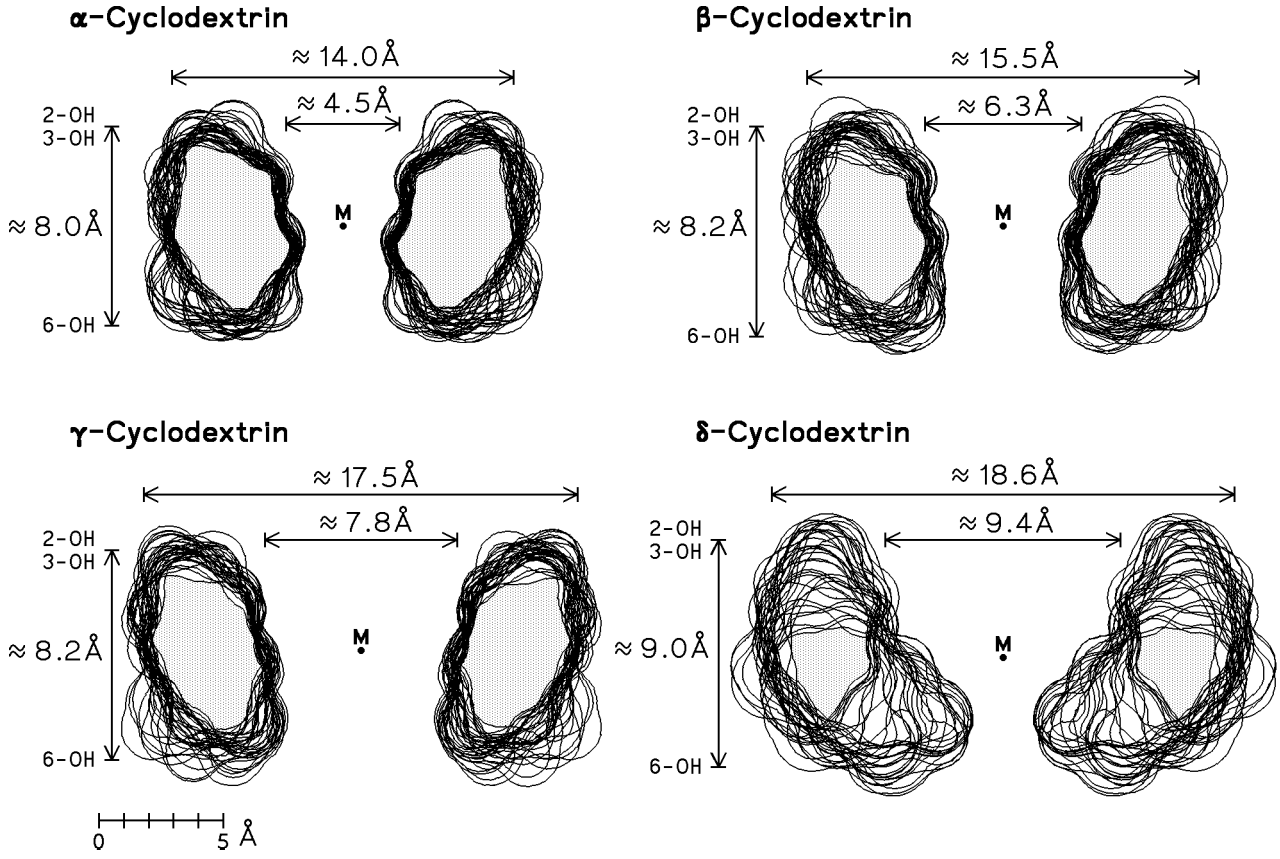

Fig. 6-8. Cross section plots (cf. Fig. 6-7) through the contact surfaces of α- (*upper left*)[339], β- (*upper right*)[344b], γ- (*lower left*)[348b], and δ-CD (*lower right*)[320,355]. The annular aperture of the 2,3-OH groups corresponds to the top sides of the contours, the 6-CH_2OH groups to the bottom faces, respectively. The approx. molecular dimensions are indicated by the various scales (*M*: center of geometry).

The irregular shaped intersection contours computed for the δ-CD are directly related to its significantly puckered macrocyclic conformation. The same holds true for the apparently increased height of the δ-CD torus of ≈ 9.0 Å, while for the other cyclodextrin classes usually 8.1 ± 0.1 Å are measured. When applying a correction to account for the large cyclodextrin puckering, the effective height of the δ-CD falls into the same range. The torsi diameters and cavity dimensions displayed in Fig. 6-8 represent a first criterion to judge the steric limitations required for the formation of inclusion complexes.

When keeping in mind some conformational flexibility of the cyclodextrins to adapt towards different shapes of guest molecules, it becomes obvious that not only small molecules such as MeOH[357], DMF[358], and DMSO[359], but also various mono- or di-substituted benzene derivatives[360] and inorganic metal complexes[323] fit well into the α-CD cavity. β-Cyclodextrins are able to include aromatic compounds carrying sterically more demanding substituents like 4-*t*-butylbenzyl alcohol[361], 4-*t*-butylbenzoic acid[362], and 4-*t*-butyltoluene[363], for example, or even spherical shaped guests like hexamethylenetetramine[364], adamantane[365] or substituted derivatives therefrom[366]. γ-CD can accommodate almost perfectly round-shaped 12-crown-4 ether complexes[367,368] (*vide infra*), or even such crowed compounds like 1,2,3-tri-*t*-butylnaphthalene[369]. In a very recent study the ability of γ-CD to form 2 : 1 inclusion complexes even with C_{60} ("Buckminsterfulleren") was outlined[370]. For δ-CD no inclusion complexes have been studied by solid state analysis so far, but on the basis of its dimensions it was concluded that napthalene would be "included loosely or rather freely, and an anthracene seems to fit well in the δ-CD cavity"[320].

Molecular Lipophilicity Profiles of Non-Complexed Cyclodextrins

Hydrophobic effects[116,117] were adduced to represent the major driving force governing the formation of inclusion complexes by cyclodextrins[306-308]. On the basis of hydrophobic interactions, appropriately sized small organic molecules are included in the hydrophobic cavity of the different cyclodextrins. In a consequent further development of this concept, it seemed appropriate to apply the methodology of Brickmann *et al.*[58] to calculate **m**olecular **l**ipophilicity **p**atterns (**MLP**'s) on molecular surfaces and visualize them in color-coded form on solid contact surface models (derived from the dotted representations, cf. Fig. 6-6) by using the MOLCAD-molecular modeling program[48]. Accordingly, the relative MLP's for the four different non-complexed cyclodextrins are shown in Fig. 6-9, with blue colors as a reminder of water corresponding to hydrophilic surface regions, while oily yellow-brown colors designate the most hydrophobic areas.

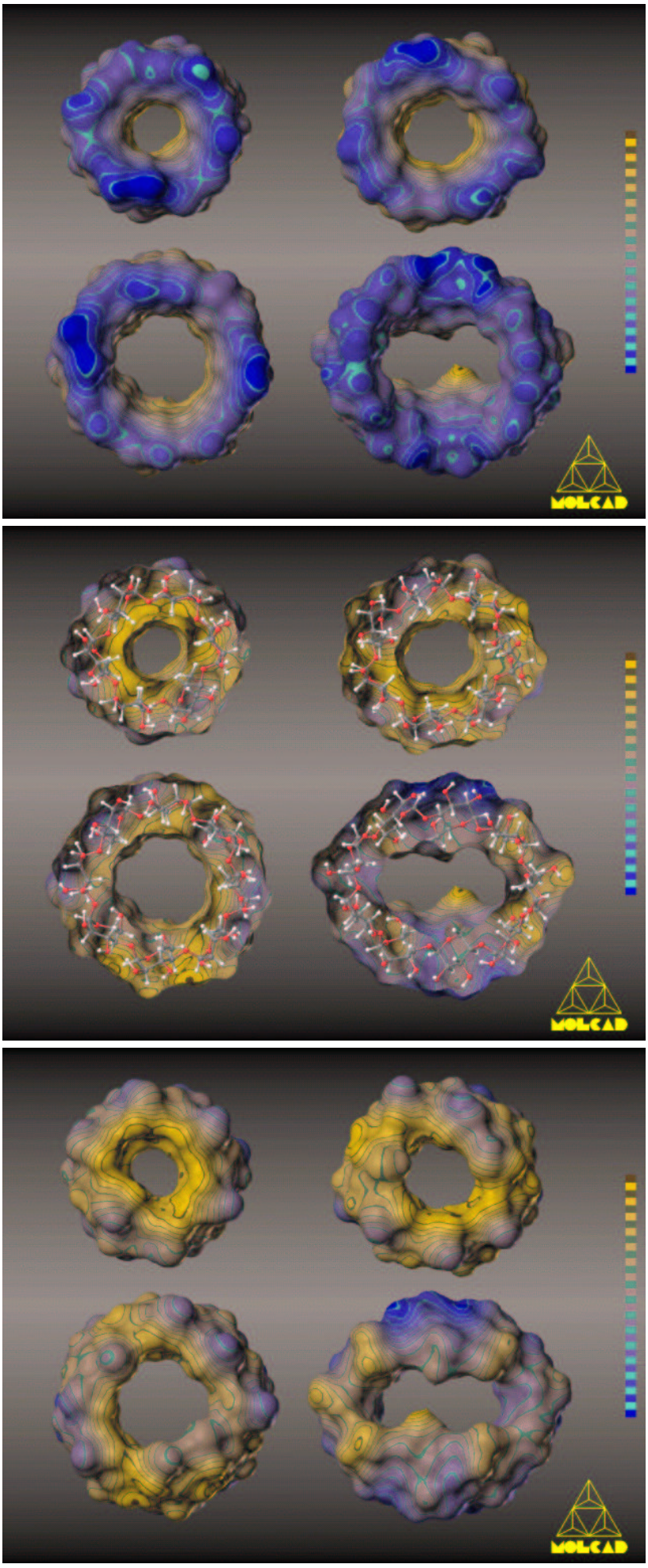
MOLCAD
MOLCAD
MOLCAD

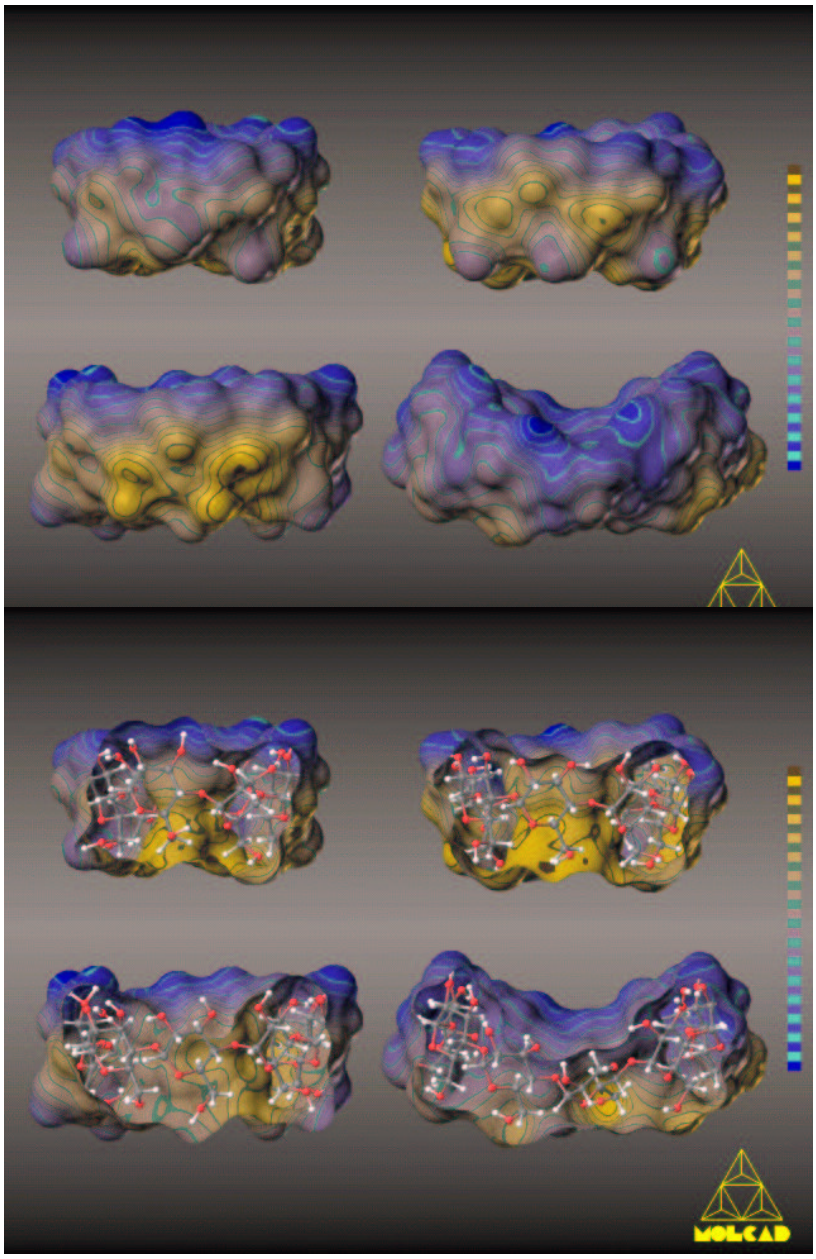

Fig. 6-9. (this and opposite page) Molecular lipophilicity patterns (MLP's) projected onto the solid state structure derived contact surfaces of the non-complexed forms of α- (*upper left*)[339], β- (*upper right*)[344b], γ- (*lower left*)[348b], and δ-CD (*lower right*, respectively)[320,355]. Blue colors indicate the most hydrophilic surface regions, while oily yellow-brown colors designate the most hydrophobic surface areas in all cases (cf. footnote on p. 75). Albeit the calculated range of hydrophobicity values (in arbitrary units) does not differ significantly for the various cyclodextrins, the color code was adapted to the MLP-range for all molecules separately (private mapping). On the *left* page, the *top* picture displays the hydrophilic (blue) large-opened 2-OH / 3-OH aperture of the cyclodextrins (cf. Fig. 6-6). In the *middle*, the hydrophilic "front" half of the surfaces has been removed providing an inside-view onto the hydrophobic (yellow-brown) "backside". The ball and stick models inserted illustrate the molecular orientations. The *bottom* representation shows the hydrophobic (yellow-brown) "backside" (rotation by 180° around a vertical axis) of the four cyclodextrins, i.e. the smaller opening carrying the 6-CH_2OH groups. On the *right* page, the side view MLP's are depicted in closed (*top* entry) and bisected (*bottom* picture) form, respectively. In all cases, the 2-OH / 3-OH side (larger opening) of the cyclodextrins is aligned upward and the 6-CH_2OH side (smaller aperture) points downward. The differences in hydrophobicity of the opposite sides are apparent, the hydrophobicity of the 6-CH_2OH side extending well into the central cavity.

The molecular images of α-, β-, γ- and δ-CD provided in Fig. 6-9 display striking similarities between the cyclodextrins of different ring size. The backside of all models is related to the primary hydroxyl groups in each case. The characteristically enhanced hydrophobicity of this molecular side is caused by the close spatial arrangement of the 6-methylene protons and the O_5-C_5-H_5-fragments of all glucose residues. Due to the accumulation of twice as much secondary hydroxyl groups the wide opened opposite rim of the cyclodextrins is significantly more hydrophilic. Because of the considerably large puckering of the macrocycle and the irregular tilting of the glucose moieties, the separation of hydrophilic and hydrophobic surface areas on the front- and back-side becomes less pronounced for the largest ring homolog, the δ-CD.

Out of the calculated total surface area of ≈ 120 Å^2 per glucose unit (α-CD: 720, β-CD: 845, γ-CD: 960, and δ-CD: 1060 Å^2) approximately 10 % contribute to the inner surface of the central cavity (α-CD: 85, β-CD: 105, and γ-CD: 140 Å^2, for δ-CD no exact value can be obtained). Most notably, it is invariably this inner area of the molecular surface which is calculated to be the most hydrophobic part in all cases. However, it should be noted that only relative hydrophobicity profiles are shown here, and no absolute values are discussed. Of course, *in toto* the cyclodextrins represent considerably hydrophilic host molecules, but nevertheless, the least hydrophilic – i.e. the most hydrophobic – surface areas are located inside their cavities.

The Thermodynamic Fundamentals of Inclusion Complex Formation

After the first interpretation of Freudenberg *et al.* of the cyclodextrin complexes being formed by molecular inclusion[371], a large body of experimental data gave rise to the (sometimes highly speculative) proposal of many different mechanisms leading to the formation of cyclodextrin 1 : 1 inclusion complexes and various origins of the molecular interactions were suggested in the literature[372]. The fact that cyclodextrins are able to form stable complexes with a large variety of compounds with entirely divagating chemical structures indicates that common properties of the system – i.e. the cyclodextrin itself and the (aqueous) solvent – rather than specific structural features of the guest must contribute most to the driving force governing the complex formation.

By means of the highly distorted solid state structure observed for α-CD · 6 H_2O (form I[337] and II[338]) Saenger *et al.* suggested an "induced-fit"-type mechanism for the inclusion process by this compound[318,337a,338,339]. In aqueous solution and prior to complex formation, this tensed hydrated "empty"-CD structure undergoes a conformational transition towards a round-shaped and more symmetrical "relaxed" geometry. The solid state form III[339] (cf. Fig. 6-6 and 6-9) was considered as a model for this "transition state", in which the water molecules within the center cavity are no

longer hold in fixed positions, but rattle in disordered locations. Replacement of this "activated" high-energy water finally results in the formation of the inclusion complex. Thus, the main part of the driving force primarily originates from relief of steric strain inherent in the α-CD. The more symmetric α-CD structure obtained from high pressure inclusion of the noble gas krypton – with a van der Waals diameter of ≈ 4.0 Å krypton is comparable in size with a water molecule – in which the Kr atom also fits only loosely the cavity with a statistical positional distribution[373] was taken as an additional fortification of this proposal[373], it also displays the flexibility of α-CD to adapt its conformation to different guest molecules. It was noted that an analogous "induced-fit" mechanism does not apply to β-[342a,c] and γ-CD[347,348], since the corresponding solid state geometries are already almost symmetrical. Also, more detailed studies[374] and the small effects of partial methylation on the stabilities of α-CD complexes indicated that the release of strain energy does not contribute significantly to the overall energetics of binding[375]. However, it was not excluded that in all cases the release of ("activated") water with its deficiency to form stable hydrogen bonds within the cavity into the bulk phase water might play a role.

By analysis of a comprehensive thermodynamic process comprising dehydration of the cyclodextrin and release of the water into the bulk phase, desolvation of the guest and relief of its hydrophobic solvation sphere, and finally the formation of the complex, an early computational study doubted the strain-releasing mechanism[376]. Instead, van der Waals interactions and the water clusters were claimed to represent the most important factors[376]. Moreover, studies on the binding characteristics of *p*-nitrophenols amplified the importance of dipole / induced-dipole interactions (London dispersion forces) for the inclusion process[377]. From measurements of ^{13}C-NMR chemical shifts and their apparent correlation with the enthalpies of complex formation, it was concluded that these dipolar interactions represent the main binding force in these processes[378]. The important role of polar effects and charges[374] is even furthermore substantiated by the fact that cyclodextrins are able incorporate large polarizable inorganic anions in their cavities[379]. Linear relationships between complex stability and the partition coefficient of the guest substrates in the water / *n*-octanol system – log *P* values, which are usually considered as an estimation for hydrophobicity[380] – and an inverse correlation of the inclusion adduct stability with the solubility of the guest in water must be considered as direct hints for the involvement of hydrophobic interactions upon inclusion[381]. In addition, changes in the UV spectra of the guest molecules are similar to the effects caused by changes of the solvent from pure water to less polar ones[382].

Enthalpy-Entropy Compensation

However, hydrophobic interactions are generally characterized as entropy driven processes, with the enthalpy contributing only to a minor extent to the total free energy change. Almost the opposite situation holds true for the inclusion complex formation of the cyclodextrins: although the experimental $\Delta H°$ and $\Delta S°$ values cover a quite broad range of values, for many guest molecules an usually large gain in enthalpy is accompanied by a compensating unfavorable (negative) entropy term[307] – a plot of the thermodynamic data adapted from Ref. [307] is given in Fig. 6-10. This so termed "atypical" hydrophobic interaction was attributed to the release of "high energy" water (*vide supra*) on one hand side, and to the opposite entropy trends of releasing hydrophobic hydration water and formation of the adduct on the other side[314]. The further reaching conclusion that hydrophobic effects might even play a minor role only[378], seems untenable, since the binding of the guests is much less strong in other solvents than pure water[383-386]. It is obvious that a strong solvophobic interaction can only occur if the solvent is more polar than the interior of the cyclodextrins. A detailed study of the solvent effects on the inclusion of indole in β-CD indicated that the complex stability is directly correlated with the surface tension of the solvent mixture, rather than with its dielectric constant[384]. The careful interpretation of the UV-spectra of the complexed indole also resulted in the conclusion that the cyclodextrin cavity closely resembles an alcohol-like environment[384].

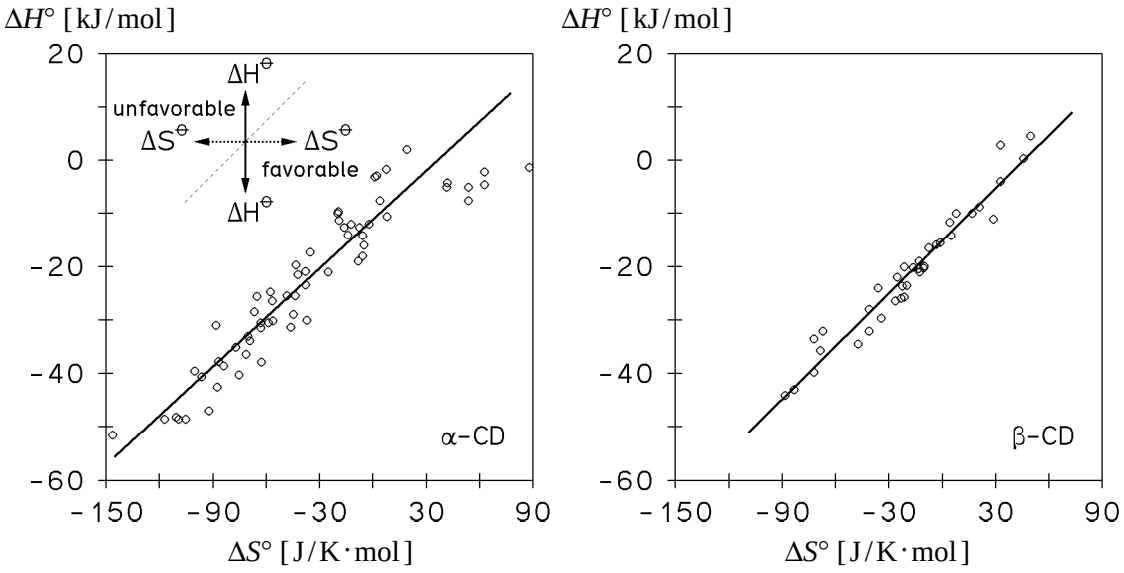

Fig. 6-10. Plot of the thermodynamic parameters $\Delta H°$ versus $\Delta S°$ for the formation of various inclusion complexes of α-CD (*left* plot) and β-CD (*right* diagram, data taken from Ref. [307]), the enthalpy-entropy compensation is indicated by linear regression, the compensating temperatures (i.e. the slopes $\Delta H°/\Delta S°$) were calculated to be $T_c = 273 \pm 14$K for α-CD, and 330 ± 13K for β-CD[307].

The phenomena described above can be easily reconciled with a recent reappraisal of the molecular origins of the hydrophobic effect[117]. Encapsulation of apolar guests in the hydrophobic interior of a macrocyclic host is usually accompanied by a complete (or at least partial) loss of the hydrophobic hydration sphere of both the guest molecule and the cavity. The general observation of the enthalpy / entropy compensation in the thermodynamic data of a large variety of cyclodextrin complexes was indeed attributed to considerable changes in the solvation of the participating molecules during molecular association[307], thus indicating the dominating role of solvation and of the thermodynamic properties of the hydration shells[387]. Water molecules within the hydrophobic hydration shells have a less favorable Gibbs energy than bulk water molecules, but it seems misleading to relate this to the general picture of somehow "ordered structures" of water molecules in distorted, clathrate-like solvation cages within the hydrophobic hydration spheres. The entropic contributions to the hydrophobic effect are related in a linear fashion to the number of water molecules in the first hydration shell, while the enthalpic changes of the hydrophobic effect can be attributed in full extent to favorable water-solute interactions[388]. The solvation of apolar solutes is mainly hampered by the extremely small molecular volume of water and the accompanying unfavorable entropy for the solvent to form an appropriate "cavity" to accommodate the solute[117], rather than by structure enhancing effects of the solute in the liquid water phase[117,388]. The contribution of this "cavity" in the solvent structure to the solvophobic effect is indeed approximately proportional to the cavity surface area and the solvent surface tension[117,381]. Thus, the total Gibbs energy of the system comprising the CD, the substrate, and the solvent, decreases when the cyclodextrin-cavity / solvent and substrate / solvent-interfaces are diminished[383]. In other words, the hydrophobic effect squeezes the cyclodextrin and the guest together to form a tight fit.

It is must be regarded as a general fact that water possesses the unique property to "amplify" the molecular recognition of even very flexible apolar groups[389]. It is noteworthy that the contribution of the hydrophobic effect is generally proportional to the area of the interacting and overlapping surface areas[148], and thus strongly depends on the depth of penetration of the substrate into the cyclodextrin cavity. On the basis of the linear relationship between the free energy change of binding with the product of the overlap surface areas during association and the surface tension of the solvent, as well as the correlation of the Gibbs energy with binding constants (Boltzmann's law), the effective overlap area of a phenyl ring with the cyclodextrin binding site was estimated to be ≈ 71 $Å^2$[381]. This value is not only in good agreement with the calculated surface area for an approximately cylindrically shaped cavity of

appropriate dimensions ($\approx 95\,Å^2$)[381], but also with the area calculated via exact integration over the Connolly surface (*vide supra*).

There still prevail some unexplained differences in the relative magnitudes of the "macroscopic" hydrophobic effect of approximately $\approx 300\,J/mol \cdot Å^2$ as estimated from surface tensions at hydrocarbon-water interfaces, and the "microscopic" effect of $\approx 200\,J/mol \cdot Å^2$ for the removal of hydrocarbon surface area from exposure to water as obtained from aqueous solubilities and partition equilibrium data[149]. The former increased value might display a considerable degree of cooperativity even of weak effects in bulk phase interactions[390], while the latter one is being well in accord with the hydrophobic effect extracted from partial free energy changes in a dipetide-antibiotic binding study[391]. Even when taking the lower limit of this area-normalized hydrophobic effect into consideration, a total overlap region of only $75\,Å^2$ will contribute with $\approx 15\,kJ/mol$ to the cyclodextrin-guest interaction. This low-boundary estimation indeed indicates that the contribution of the hydrophobic effect to the overall energetics of binding is by no means negligible.

The afore mentioned enthalpy / entropy compensation in the binding of substrates to cyclodextrins (cf. Fig. 6-10) may not only be a consequence of the unique solvation properties of water since similar compensation phenomena are not limited to (aqueous) solutions, but are observed for many entirely different processes[392,393]. The slope of the $\Delta H°/\Delta S°$ regression curves in Fig. 6-10 is termed the "compensating temperature", at which idealized substrates independently of their chemical structures should bind with uniform strength to the cyclodextrin cavity. At lower temperatures the effects of $\Delta H°$ on the complex stabilities should become more important, and *vice versa*, higher temperatures would lead to an enhanced significance of entropic effects and $\Delta S°$. Only rather small fluctuations of the experimental data around perfect linearity indicate the intricacies of chemical structures involved in the inclusion complex: deviations towards the upper left corner of each plot reveal both more unfavorable enthalpic (vertical direction) and entropic effects (horizontal deviations) in the complex, while dispositions towards the lower right corner are synonymous to more favorable values of $\Delta H°$ (vertical) and $\Delta S°$ (horizontal direction) when compared with the parameters obtained from the idealized linear relationship.

An impressive and straightforward explanation for these compensation effects was provided by Williams *et al.*: large enthaplic effects usually originate from strong (e.g. electrostatic) interactions between polar compounds. However, the price to be paid for strong forces trying to stabilize a well-defined configuration of an associated complex, is a severe restriction of disorder and molecular motions in the assembly, which in consequence must lead to a large unfavorable (negative) entropy contribution[393].

Provided that the basic molecular mechanism of the (association) process does not change significantly for various ligands, both the enthalpic and entropic effects compensate each other more or less efficiently, and in turn, level off differences in the chemical structures of the substrates to some extent.

Obviously, the compensating effects are not only observed for small chemical changes in the substrates – as evidenced for example by the wide-spread diversity of chemical structures which are able to bind to the cyclodextrins and which were included in Fig. 6-10 – and over small ranges of $\Delta H°$ and $\Delta S°$ values only, but represent a concept of almost general validity in molecular recognition[393]. The coverage of large $\Delta H°$ and $\Delta S°$-ranges in Fig. 6-10 implies that in future it cannot be expected to discover "high-potency" substrates, which exceed the common range of binding constants towards the cyclodextrins by several orders of magnitude.

As indicated by the usually observed loss in entropy upon complex formation, the favorable entropy contribution of releasing hydrophobic hydration water and the decrease of the "solvent-cavities" which contained both the participating solutes, cannot compensate the loss of translational and rotational degrees of freedom for the substrate during encapsulation. The gain in entropy detected for example in the complexation of primary alcohols with β-CD[307] might be related to an imperfect steric fit, retaining some motional degrees of freedom of the guest inside the cavity. Also, inclusion of exceedingly hydrophobic adamantane derivatives shows an increase in entropy[394] as expected for a "typical" hydrophobic behavior. However, it must be noted that the signs of $\Delta H°$ and $\Delta S°$ alone should not be over-interpreted[384].

Enthalpic contributions not only originate from the destruction of hydrophobic hydration, but it must be expected that significant effects are also provided from favorable van der Waals interactions, electrostatic forces, permanent and induced dipole-dipole interactions, polarization effects, and London dispersion forces, as well as from hydrogen bonding interactions in these complexes[115]. Intermolecular hydrogen bonds were considered to be not very important, since cyclodextrin derivatives which are not capable to act as hydrogen bond donors (e.g. per-*O*-methylated cyclodextrins) still exhibit a considerable complex formation ability. Nevertheless, H-bond interactions between cyclodextrins and included guest molecules are observed in many solid state structures[192,323,357-364,366], and therefore it might be misleading to entirely neglect their relevance. A very recent force field based analysis of the complexing behavior of γ-CD towards various substituted dimethoxy-benzyl *t*-butyl ketones in alternating orientations, claimed van der Waals interactions to mainly control the inclusion complex. The poor agreement with experimental data originates (at least partially) from an entirely unjustified computational procedure (i.e.

MM instead of MD-calculations and comparison of single-geometry structural energies only). The implicit exclusion of solvent molecules by the MM methodology applied, does not allow for an estimation of the hydrophobic effect, which must definitely be regarded as a solvent-induced effect[350].

Obviously, far more than one single effect contributes to the stability of the cyclodextrin inclusion complexes. The by far most important prerequisite for complex formation is the fulfillment of steric requirements and the spatial fit of the guest into the host cavity.

In the past, it was seemingly entirely ignored that many basically weak interactions are strengthened to a considerable extent by their simultaneous action[390]. Williams *et al.* indeed showed experimentally that electrostatic and hydrophobic interactions enhance themselves in a cooperative way, i.e. the overall effect is significantly greater than the sum of the individual parts, even when special care is applied to take the classical chelat effect into consideration[395].

In summary, the molecular modelings provide further fortification for hydrophobic interactions being of paramount importance in the process of the inclusion complex formation. The afore mentioned direct relationship between the complex stability and the partition coefficients of the substrates in the water / *n*-octanol system[381] sheds further light onto the meaningfulness of the hydrophobicity profiles presented in Fig. 6-9, since fragmental atomic contributions[145,146] to these log *P* values represent the computational basis for the calculation of the MLP's[58]. The multitude of many undirected and unspecific non-covalent interactions contributes with varying significance to the molecular recognition capability of cyclodextrins, and to the molecular self-assembly of the inclusion complexes. Blokzijl *et al.* have outlined the current dilemma to distinguish and to separate dispersion forces and hydrophobic interactions analytically[117], but it is clearly evident that both are of fundamental importance for assessment of the physico-chemical properties of the cyclodextrins. On the other hand, conformational flexibility must also have a pronounced effect on the stability of cyclodextrin complexes. Thus, on the basis of the distorted solid state structure of δ-CD[320] and its MLP (Fig. 6-9), it is to be expected that lowered complex stabilities should be found for this CD, and this should apply even more to its larger homologs.

The Hydrophobic Topographies of Cyclodextrin Inclusion Complexes

The fundamental importance of the MLP's of the non-complexed cyclodextrins, for providing new insights into the inclusion process itself, now raises the pivotal question, inasmuch they also have impact on the orientation by which guest molecules

are incorporated into the cavity. As evidenced by numerous NMR-investigations and solid state structures, the asymmetric and regiospecific penetration of the guest molecules seems to be a general phenomenon[377]. Obviously, the phenolic OH-groups of various *p*-nitrophenols cannot penetrate the cyclodextrin cavity either for solvation reasons, or the substrate dipole has strong orienting preferences[360c,377]. In solution *p*- and *m*-nitrophenolate approach the cavity with the nitro group first (i.e. pointing towards the 6-CH_2OH groups), due to steric hindrance the latter guest being less deep incorporated than the former one[396]. The large dipole moment of α-CD being directed from the 2,3-OH (negative end) groups towards the 6-OH (positive side) seems to determine the orientation of guest molecules in the cavity, such that they are included with high preference towards the antiparallel alignment of the individual dipole moments[397]. Deprotonation of the OH-group of the phenols affects the complex stability to a less pronounced extent than deprotonation of the cyclodextrin (destabilization of the macrocycle and the hydrogen bonding network between the 2- and 3-OH groups, *vide supra*)[398]. Within a large variety of different *p*-substituted phenols, the degree of insertion seems to vary only to a little extent, with the guest molecules fitting deeper into the wider cavity of β-CD than that of the narrower α-CD[398]. By means of molecular mechanics calculations the van der Waals interaction, and thus the quality of the steric fit, was considered as a good estimation for the relative complex stability amongst similar guest molecules like various regioisomeric nitrophenols and nitroanilins[399]. As evidenced by line-shape analysis of ^{13}C-CP-MAS solid state NMR data, the guest molecules can undergo some motions inside the cavity, the extent of which depends on the cavity diameters, and thus is considerably lower in the α-CD complexes than in the β-cyclodextrins[400,401]. For *p*-nitrophenol an activation energy of about 50 kJ/mol was measured for the motion inside the cavity. The exact value strongly depends on the degree of hydration of the crystal and suggests that the conformational flexibility of the inclusion complexes generally increases in solution[401].

The geometry of the inclusion complexes in not necessarily the same in the crystalline state and solution. This is demonstrated, for example, by a comparison of the orientation of the guest in the X-ray structure[402] and the NMR-derived solution conformation[403] (note also the different conclusions drawn from the experimental facts in Ref. [396] and [403]) in the α-CD *m*-nitrophenol inclusion complex. Notwithstanding this fact, in the sequel some solid state structures should be used to elucidate the fundamental principles of how the regiospecificity of encapsulation can be related to the relative hydrophobic characteristics of both the host and the guest.

The Hydrophobic Guest-Host Relationship as Exemplified for α-Cyclodextrin Inclusion Complexes

As a typical example, the crystal and molecular structure of the α-CD *p*-iodoaniline trihydrate 1 : 1 inclusion complex was studied by X-ray structural analysis[360a,404], and one unit of the complex is shown in Fig. 6-11 in combination with the individual contact surfaces of the guest and the host. *p*-Iodoaniline is deeply buried into the α-CD cavity with the iodine atom pointing towards the primary 6-OH groups, while the amino grouping sticks out on the opposite aperture without being hydrogen bonded to the host. All glucose residues (uniform $^4C_1$-shape with CP-parameters $<Q> \approx 0.57(3)$ Å and $<\theta> \approx 5(3)°$) are canted with the primary hydroxyl groups towards the center of the molecule ($\tau \approx 91 - 106°$, $<\tau> \approx 99(4)°$), with all 6-CH_2OH-units adopting a *gg* conformation except of one disordered one. The macrocyclic perimeter itself is puckered to a minor extent only (torsions $|\theta_{O\text{-}O}| \approx 1.8 - 7.4°$, $<|\theta_{O\text{-}O}|> \approx 4.7(1.9)°$ and O_1n-deviations from planarity of ≈ 0.08(4) Å). Cramming the phenyl ring into the α-CD leads to a pronounced elliptical distortion of the macrocycle with O_1-$O_{1n'}$-distances of 8.15 – 8.85 Å ($<d(O_1\text{-}O_{1n'})> \approx 8.5(3)$ Å) and $d_{min}/d_{max} \approx 0.92$. The longest O_1-$O_{1n'}$-axis is paralleled by the aromatic ring, while the long C_1-C_4-axis of the phenyl ring is thereto almost perpendicular and coincides approximately with the *pseudo-*C_6-symmetry axis of the α-CD.

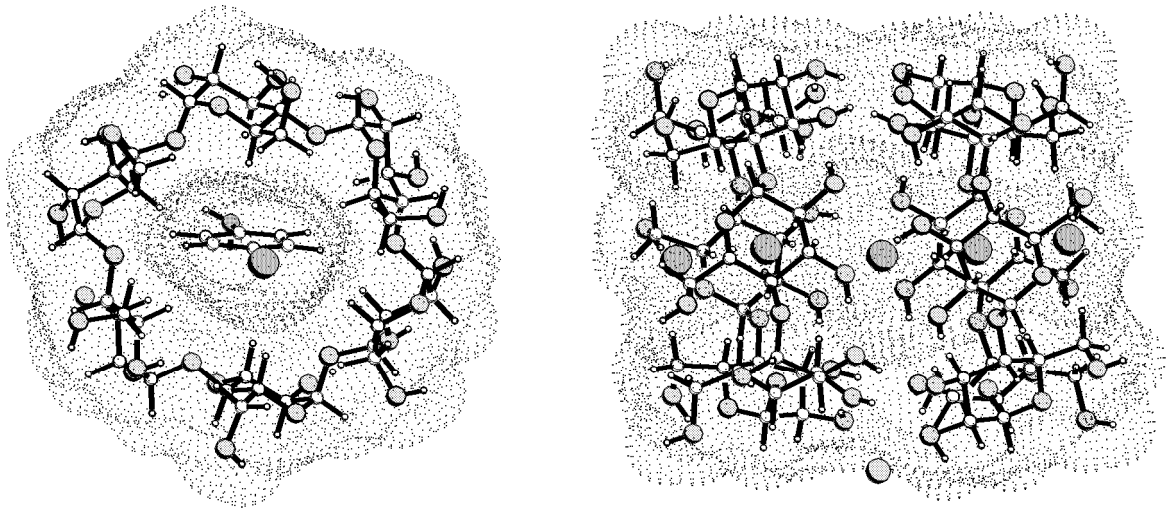

Fig. 6-11. Ball and stick models and Connolly surfaces of one formula unit of the α-CD *p*-iodoaniline trihydrate inclusion complex[404] (*left* side, view from the 6-CH_2OH side and approximately perpendicular to the cyclodextrin mean plane), and the $(\alpha\text{-CD})_2 \cdot LiI_3 \cdot I_2 \cdot 8\ H_2O$ adduct[405] (*right* model, projection perpendicular to the axis of the channel formed by both cyclodextrin units), in both cases, the water of crystallization was removed.

The perfect steric fit of the guest inside the cavity is even better illustrated by the cross section plots given in Fig. 6-12 and the solid surface models – note in particular the side views – shown in Fig. 6-13, than by the dotted representations.

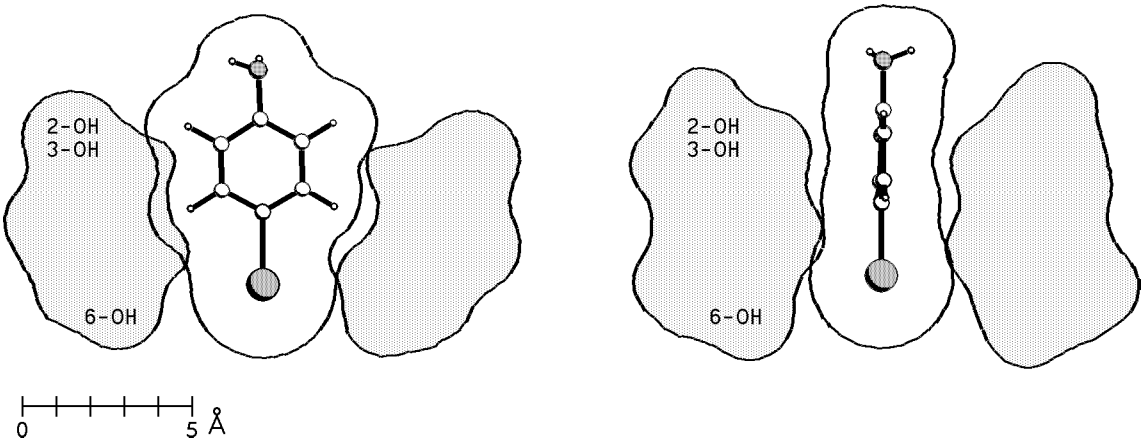

Fig. 6-12. Surface cross section through the center of geometry of the α-CD *p*-iodoaniline inclusion complex[404] parallel (*left* side) and perpendicular (*right* plot) to the phenyl ring of the guest. Beside the perfect steric fit, the elliptical distortion of the cyclodextrin ring according to the flat disc-shape of the phenyl ring becomes evident.

In Fig. 6-13, the usual color-code was applied to visualize the lipophilicity pattern for the inclusion complex. Note the different modes of scaling (left and right part) in Fig. 6-13: the first color-scale (left part of Fig. 6-13) was adapted to each molecule individually to illustrate the close spatial relationship of hydrophilic and hydrophobic surface regions of the guest and the host molecule ("private scaling"). The second scale (right part) was chosen to demonstrate the entirely different absolute values of hydrophobicity (in arbitrary units), and of course, *p*-iodoaniline is much more hydrophobic than the α-CD is ("absolute scaling"). This mode again reflects the hydrophobic effect to contribute – to an at least important part – to the driving force for the formation of the inclusion complex, by diminishing the interface area of the solvent with the aromatic ring and the iodine atom. Most notably from the relative-scaled models – in particular from the side-view models where the surface has been partially sliced – is the excellent conformity of the most hydrophilic and the most hydrophobic surface regions on the guest-host interface, i.e. the hydrophobic iodine atom is located close to the 6-CH_2OH groups and the amino function points towards the hydrophilic parts of the cyclodextrin ring. This correlation is not only limited to this complex geometry shown here, but it also applies to many other inclusion complexes.

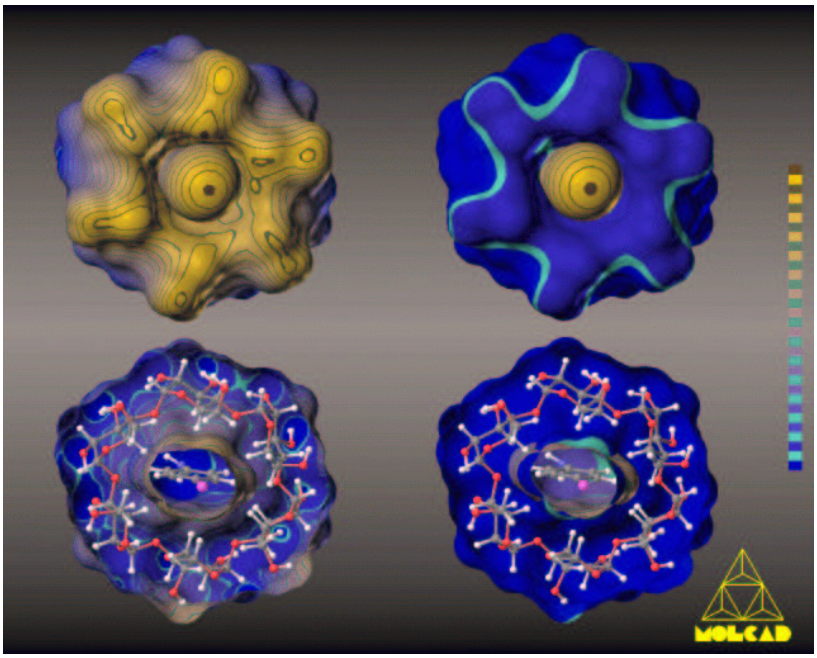
MOLCAD

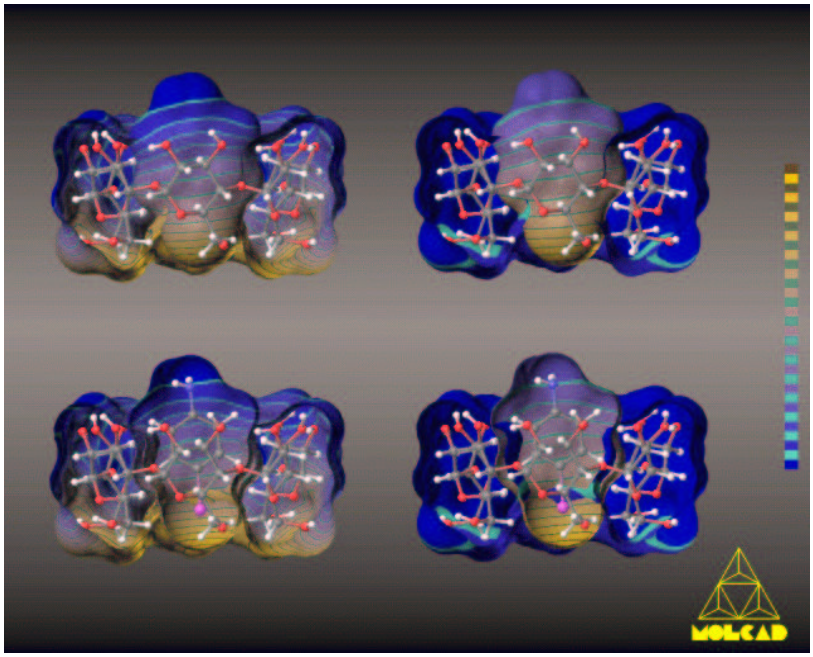
MOLCAD

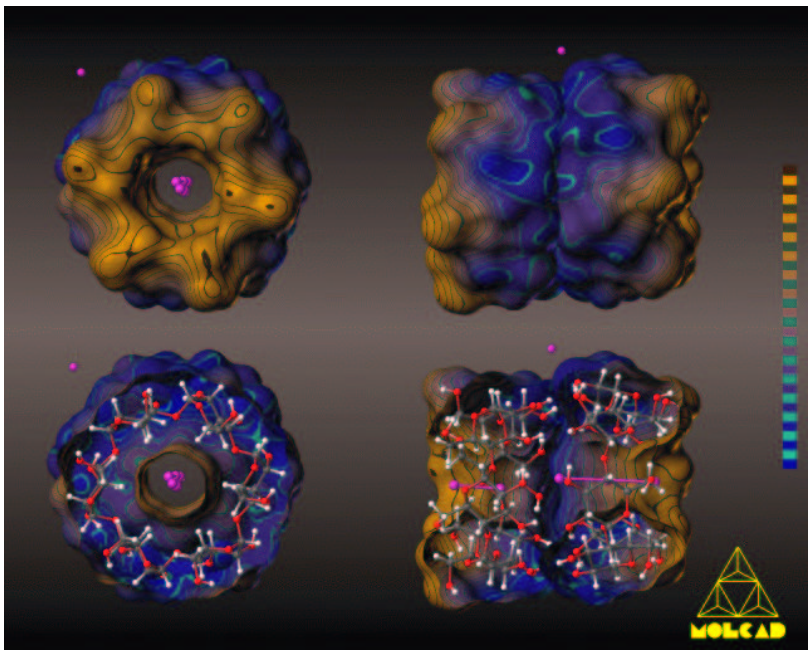
MOLCAD

Fig. 6-13. (opposite page, *top* and *center* picture). The lipophilic topography of the α-CD *p*-iodoaniline trihydrate inclusion complex[404] (blue colors correspond to hydrophilic regions and yellow-brown to hydrophobic surface areas). The water molecules of crystallization were removed and the MLP's were calculated on the individual surfaces for each of the isolated molecules separately, which were reassembled to the complex. In the *top* entry, models are shown with the 6-CH_2OH cyclodextrin-aperture facing the viewer, in closed and half-opened form, respectively. The *lower* picture displays side view models with two different depths of surface slices. In the *left row*, the color-code was adapted to the individual molecules separately (private mapping), thus pointing out the almost perfect alignment of most hydrophobic and hydrophilic regions (in relative terms) between the guest molecule and the host cavity. In the *right row*, coloring was performed by using the absolute range of MLP values (in arbitrary units) over both molecules as the common standard. Apparently, the *p*-iodoaniline guest is much more hydrophobic than the cyclodextrin is, yet the MLP's sustain the notion that the relative distribution of hydrophobicity on the interface of both surfaces controls the regiospecificity of incorporation and the relative orientation of the guest molecule inside the cavity.

For example, in the solid state clathrate structures of α-CD and benzaldehyde[406], sodium 1-propanesulfonate[407], sodium benzenesulfonate[360b], *m*-nitroaniline[360d], 1-phenylethanol[360e], β-CD and ethanol[352] or benzyl alcohol clathrate[408], and γ-CD 12-crown-4 ether complexes[367,368] (*vide infra*), the most hydrophilic molecular parts of the guest point towards the secondary 2,3-hydroxyls, whilst the hydrophobic regions are invariably projected straight into the cavity.

However, in some crystal structures of inclusion complexes like α-CD 3-iodopropionic acid[409] and 2-pyrrolidone[359], as well as β-CD 1-hydroxymethyl-adamantane[366], 4-*t*-butylbenzyl alcohol[361] and 4-*t*-butylbenzoic acid[362] clathrate an inverse guest-host relationship is observed than would be expected from the hydrophobicity patterns. Either the afore mentioned tendency to avoid interactions between parallel aligned dipoles, or the absolute necessity to fulfill steric requirements as displayed by bulky groups which avoid the narrow aperture of the CD, can overcome the guest-orienting force of the molecular hydrophobic topographies.

Fig. 6-14. (opposite page, *bottom* picture). Cyclodextrins as simple models for the starch-iodine complex: molecular lipophilicity pattern (MLP) for one formula unit of the $(\alpha\text{-CD})_2 \cdot LiI_3 \cdot I_2 \cdot 8\,H_2O$ complex[405] (the water of crystallization has been removed and only the cyclodextrin molecules were used for the calculation of the MLP's, color-coding according to Fig. 6-9). The *left* models are shown along the central channel axis and perpendicular to the cyclodextrin mean planes, while the *right* models were rotated by 90° each to illustrate the almost perfectly linear alignment of the iodine atoms inside the channel-type cavities. The lithium ion is indicated by the isolated green symbol at the *lower right* and *lower middle* position of the models, respectively.

Obviously, according to the fundamental principle "*similia similibus solvuntur*", the guest and the host tend to orient in such a way that most hydrophobic surface regions of the host are opposed by just the most hydrophobic parts of the encapsulated guest, and *vice versa*, hydrophilic parts correlate with each other, too.

α-*Cyclodextrin Complexes as Models for the Blue Starch-Iodine Adduct*

The analogous α(1→4)-type intersaccharidic linkages, the cyclic structure of the cyclodextrins, as well as their enzymatic pathway of generation by cutting out one single turn of the starch helix bring their utilization as simple model compounds for this complex natural polysaccharide close at hand. Most notably, the cyclodextrin complexes with iodine[410,411] and polyiodide[405,412-414] were considered as putative models[318] for the well-known deep-blue stained amylose-iodine-iodide complex[415]. On the basis of an X-ray diffraction fiber analysis of the dye complex, the iodine atoms were found to be located within the channel of V_H-type, single-stranded amylose. They are aligned almost co-linear to the center six-fold helical symmetry axis, exhibiting a fiber repeat distance of approx. 8.17 Å and an incongruent average spacing of ≈ 3.0 Å between the iodine atoms[416]. Since low-resolution fiber-analysis is not very reliable – and there still exist some open questions on the conformation of amylose in general[417] – the structural data obtained for cyclodextrin model-complexes must be considered as much more accurate.

Solid state structures of hydrated iodide-free α-CD · I_2 complexes with varying amounts of crystal water exhibit a herring-bone arrangement of the cyclodextrin units in the lattice with cage-type cavities rather than channels, which are blocked by contiguous molecules. The isolated iodine molecules are aligned coaxial to the cavity axis and contribute to the reddish-brown color of the crystals[410,411]. The fundamental role of water, iodine, and iodide for the formation of the dark-blue colored amylose complex has been outlined[415]. Thus, it is not surprising that co-crystallization of α-CD with various polyiodides yields dark-brown to dark-blue stained complexes, which exhibit entirely different, infinite channel-type structures with approximately linear alignments of the polyiodide ions along the central axis[405]. Most notably, the $(\alpha\text{-CD})_2 \cdot LiI_3 \cdot I_2 \cdot 8\ H_2O$ complex (Fig. 6-11) comprises two crystallographically independent cyclodextrin units which are stacked in a head-to-head arrangement along a common axis, with a slight inclination of ≈ 7° and a shift of approx. 1.1 Å in respect to each other[405]. All C_6-O_6-bonds point towards the outside of the tori (ω ≈ -60°, *gg* arrangement). The cyclodextrins are remarkably symmetrically round-shaped with low fluctuations of the tilt angles (τ ≈ 91 – 106° and $<\tau>$ ≈ 99(4)°) and O_1-$O_{1'}$-distances ($<d(O_1\text{-}O_{1'})>$ ≈ 8.5(1) Å, d_{min}/d_{max} ≈ 0.97) only, the macrocyclic perimeter is almost flat-shaped ($<|\theta_{O\text{-}O}|>$ ≈ 8.1(3.8)°, $<d_{O1}>$ ≈ 0.05(3) Å).

The iodine atoms (four ordered positions and one disordered) are embedded in the central infinite channels of this structure with non-equal asymmetric distances (mean value ≈ 3.1 Å) forming distinctly separated $I_2 \cdot I_3^-$ units, the Li^+ cation being located on the outside of the cyclodextrins and out off range of strong interactions with the anion.

The torus height of the cyclodextrins is approximately identical to the fiber repeat (i.e. the height per turn of the helix) in the amylose complex, and the average iodine-iodine distances correspond roughly to those found there. However, the MLP's calculated for the cyclodextrin complex (cf. Fig. 6-14) shed some light on the disadvantages of cyclodextrin complexes as models for starch. The generally observed head-to-head arrangement of the cyclodextrin macrocycles in the polyiodide crystals investigated[405] leads to an alternating projection of hydrophilic (polar) and hydrophobic (apolar) regions onto the wall of the channel by the 2,3-OH and 6-CH_2OH groups. Due to the "infinite" polymeric nature of amylose in which all primary and secondary hydroxyls point towards the same direction, respectively, this structural property cannot prevail in the amylose complex. Thus, a much more homogenous hydrophobic character of the amylose channel must have a considerable influence on the electronic structure of the polyiodide chain. This in turn, can account for the different color of both adducts (dark-brown *versus* dark-blue). In addition, the obvious differences in the diameters of the cyclodextrin apertures lead to a channel which is significantly buckled at the (polar) connection between neighbored cyclodextrins, where the secondary hydroxyls interact.

On the basis of the MLP's it is to be noted that cyclodextrins can be used as models for starch on a very crude and rough level only. Their asymmetry and finite torus-height must lead to considerable "end"-effects which are not present in polymer structures, and which certainly will influence the structure of inclusion complexes in a very pronounced fashion. This necessarily not only applies for the polyiodide complexes discussed here, but also to the inclusion adducts of amylose[418,419] and cyclodextrins[420] with various surfactants, for example. A detailed discussion of the hydrophobic characteristics of different types of starch and the amylose-iodine complex is given in Chapter 11.

Flexible Guest Molecules in the β-Cyclodextrin Cavity

Elongated chain-type molecules with hydrophilic head groups will tend to hide their more hydrophobic center parts from interaction with the solvent by threading into the cavity of the cyclodextrins. An illustrative example in this regard is the solid state structure of the β-CD 1,4-butanediol · 6.25 H_2O inclusion complex[421] (Fig. 6-15).

The cyclodextrin unit itself is not highly distorted and almost regularly round-shaped with glucose tilt angles around $\tau \approx 110(10)°$, O_1-O_{1^n}-distances ranging between 9.34 – 10.17 Å ($<d(O_1\text{-}O_{1^n})> \approx 9.8(3)$ Å), $d_{min}/d_{max} \approx 0.92$, and slight puckering of the macrocycle only (mean torsion $<|\theta_{O\text{-}O}|> \approx 8.0(5.4)°$ and O_{1^n}-deviations from planarity around 0.19(8) Å).

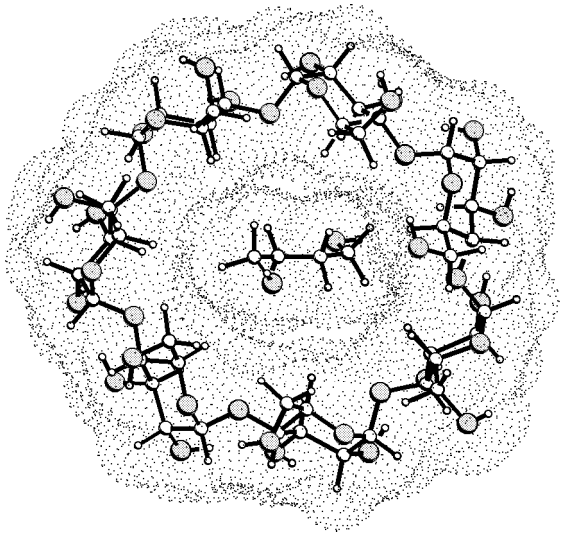

Fig. 6-15. Connolly surface and ball and stick model of the β-CD 1,4-butanediol · 6.25 H_2O inclusion complex[421] with the water molecules being left out. Due to the low atomic resolution of the structure determination for the vibrating chain ligand, only its mean atomic positions were taken into consideration.

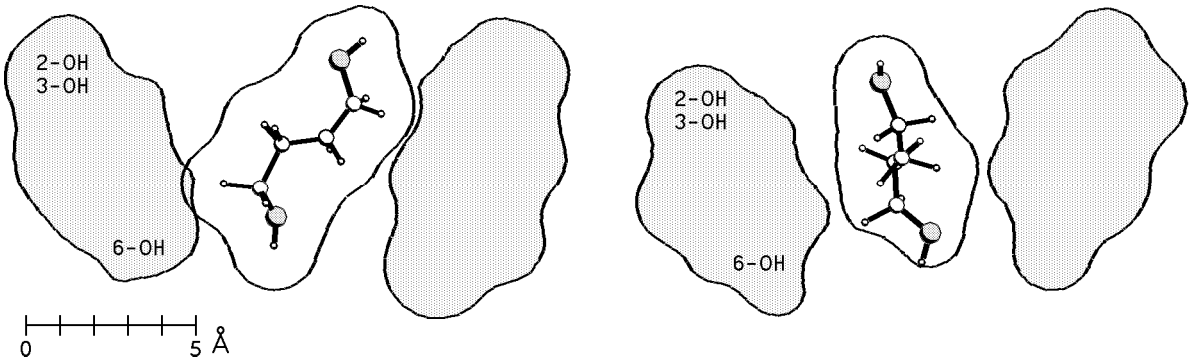

Fig. 6-16. Two mutually perpendicular surface cross sections through the center of geometry of the β-CD 1,4-butanediol complex[421], the loose steric fit displays the extended conformational space available to the ligand.

Since the cavity is much larger than the van der Waals diameter of the ligand (cf. Fig. 6-16), it vibrates extensively in its cyclodextrin cage. The atomic resolution of the structure determination did not allow to differentiate between various disordered, distinct molecular conformations of the butanediol, and thus, only the mean atomic positions of the guest could be established. In consequence, thermal averaging leads to a virtual covalent conformation of the chain, which in terms of bond length, angles, and torsion is poor and does not represent a real energy minimum conformation. The O-1 and O-4 oxygens atoms are involved in smaller thermal motions than the carbon atoms are, indicating that different chain conformations are able to hold them in a position with a fixed distance and a maximum of hydrogen bonding interactions with adjacent molecules[421]. However, for such simple molecules like 1,4-butanediol the visualization of MLP on the corresponding molecular surface is almost independent on the exact molecular conformation, as long as the proper atomic hydrophobicity parameters are taken into consideration. In both cases, the hydroxyl groups represent hydrophilic head groups, which are separated by an extended hydrophobic spacer.

As particularly evident from the MLP of the complex shown in Fig. 6-17, the polar head groups of the slightly inclined guest point through the opposite wide and narrow opened apertures of the torus. The central part of the aliphatic chain occupies the major portion of the β-CD cavity[421]. Thus, the least polar molecular parts are efficiently masked by the cyclodextrin and prevented from less favorable interactions with adjacent water molecules included in the crystal. If considering the solid state structure a "snapshot" image of the solution conformation as well, the hydrophobic component of the guest-host interaction becomes clear again. In particular the side-view models presented in Fig. 6-17 illustrate the apolar environment provided by the β-CD cavity, and its function to hide the tetramethylene unit and diminish the corresponding solute-solvent interface in (aqueous) solution.

Similar inclusion geometries and effects have been observed in the isomorphous crystal structure of β-CD ethanol octahydrate[352]. Ethanol – representing half the structural motif of 1,4-butanediol – is fixed by its hydroxyl group approximately in the plane described by all the 2-O and 3-O atoms, with the $-CH_2CH_3$ residue pointing into the cavity and vibrating considerably.

γ-CD · 12-Crown-4 Ether as an Example for a Capped Cyclodextrin Inclusion Complex

In contrast to its lower ring homologs relatively few crystal structures were reported for γ-CD and its complexes. All these structures are of high symmetry and indicate that γ-CD may be the least distorted and untensed compound within this class of cyclooligosaccharides.

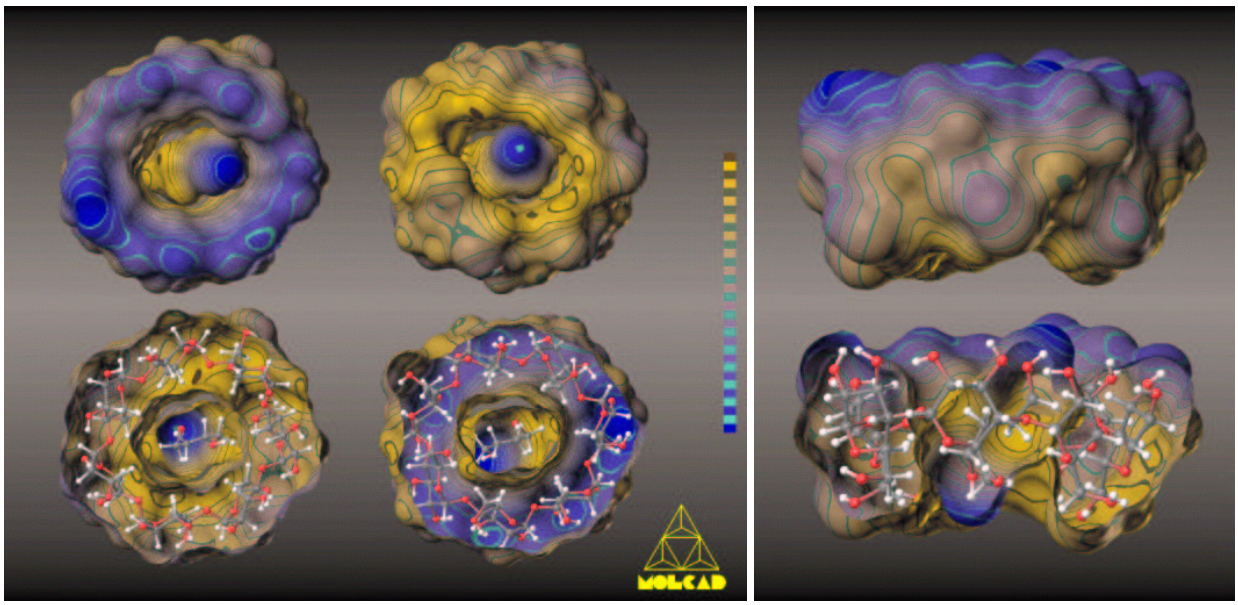

Fig. 6-17. Representation of the hydrophobic characteristics (MLP's) of β-CD 1,4-butanediole inclusion complex (mean atomic positions were used for the guest)[421] using the same color-code as in Fig. 6-9. In all models the color-scale was adapted individually to the range of values calculated for each separate molecule. The *left* models show the 6-OH side of the complex in closed and half-opened form, respectively. Rotation by 180° around a vertical axis exposes the opposite 6-OH aperture (*middle* entries). Most impressively, the side view models on the *right* with different depths of surface clipping illustrate the 1,4-butanediol to penetrate the cavity in full extent. Its most hydrophobic molecular regions (yellow-brown) are masked by the hydrophobic surface regions of the cavity in the cyclodextrin host molecule.

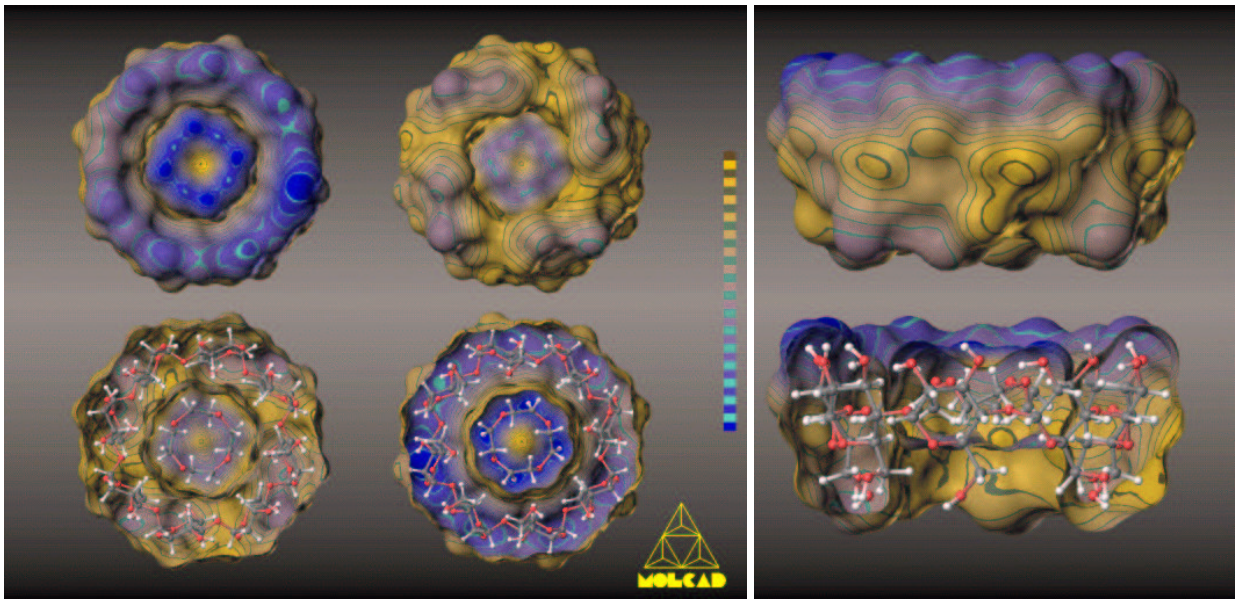

Fig. 6-19. Hydrophobic topography (MLP) of one structural subunit of the γ-CD 12-crown-4 1 : 1 inclusion complex[367], the color-code applied, the mode of scaling, and the molecular orientations shown are analogous to Fig. 6-17. The side view models again illustrate the alignment of hydrophobic and hydrophilic molecular regions on the interface between the host and the crown ether guest molecule, the latter being asymmetrically disposed close to the larger 2-OH / 3-OH opening of the cyclodextrin.

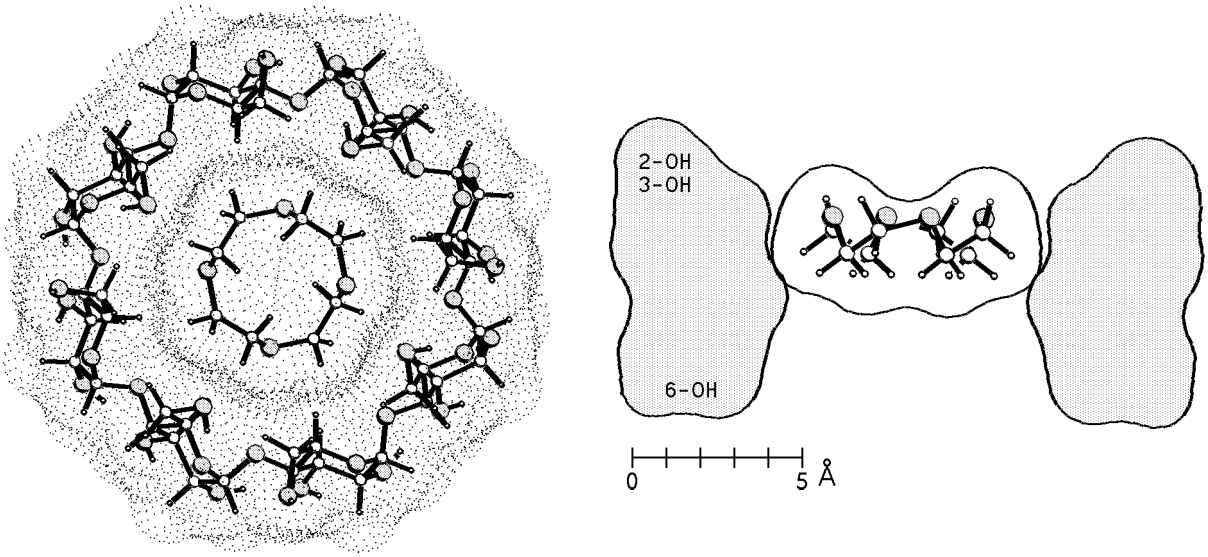

Fig. 6-18. Geometry and dotted contact surface of one γ-CD · 12-crown-4 ether unit in the salt-free solid state structure of the nonahydrate[367], the water of crystallization was removed. The *right* plot corresponds to the surface intersection with a plane perpendicular to the cyclodextrin ring and through its geometrical center. Clearly, the lid-like, asymmetric inclusion of the guest by the cyclodextrin host becomes obvious.

The inclusion complexes of γ-CD with 12-crown-4 ether[367], partially in combination with various inorganic salts[368], clearly show the guest-host geometry relationship on a good atomic resolution, all these structures being isomorphous with each other. Three crystallographically independent cyclodextrin molecules A – B – C are stacked along a C_4-symmetry axis in a head-to-tail (A – B), head-to-head (B – C), and tail-to-tail (C – A) relationship, each enclosing a 12-crown-4 moiety with an approximately all-*(-)gauche* shape of the four consecutive -O-CH_2-CH_2-O-ring units (torsion angle ≈ -93°). In Fig. 6-18, the molecular geometry of the salt-free γ-CD · 12-crown-4 ether complex is shown in combination with its dotted Connolly-type surface. The cyclodextrin torus itself is symmetrical with typically narrow distributions of the monosaccharide tilt angles ($<\tau> \approx 104(2)°$) and O_1-$O_{1^{n'}}$-distances ($<d(O_1\text{-}O_{1^{n'}})> \approx 11.75(3)$ Å and $d_{min}/d_{max} \approx 0.995$); also the parameters $<|\theta_{O\text{-}O}|> \approx 2.1(9)°$ and $<d_{O1}> \approx 0.017(8)$ Å indicate very little puckering of the whole γ-CD.

In addition, the surface cross section plot through the surface (right plot in Fig. 6-18) illustrates the crown ether moiety to be included rather shallowly with an asymmetric disposition towards the wide opened aperture of the host, the perfect steric fit evokes the picture of a lid on the inner brink of a torus.

The solid surface models provided in Fig. 6-19 emphasize even more the importance of steric complementarity as a fundamental prerequisite for the formation of guest-host adducts. The crown ether being displaced towards the wide opened end of the cyclodextrin cavity, since the opposite aperture seems to be to narrow for inclusion. As described above, the MLP visualized by color-coding on these surface models again illustrates the almost perfect conformity of most hydrophobic and most hydrophilic (note the terminology of relative terms for each separate molecule, since the "absolute hydrophobicity" of both compounds must differ significantly!) surface regions at the guest-host interface. The polar-apolar side differentiation of the crown ether moiety is caused by the spatial separation of the four ring oxygen atoms and the eight methylene units pointing towards contrary directions, and thus, contributing to opposite surface regions[367]. The hydrophobic methylene groupings are directed into the inner part of the hydrophobic cavity, while the polar oxygen atoms are located close to the hydrophilic torus rim made up by the 2- and 3-OH groups of all glucose residues. The same-side location of all ether oxygens leads to the formation of a shallow surface dent at the center of the crown guest (compare with the side-view pictures depicted in Fig. 6-18 and 6-19), which is amenable for interactions with cations. Indeed, in the γ-CD · 12-crown-4 complexes in which inorganic salts were incorporated, the cations are located in a double-decker fashion between the center of two tail-to-tail arranged cyclodextrin units, with the crown ethers providing a suitable environment for eight-fold coordination for the metal ion[368]. An analogous coordination is not possible between the head-to-head and head-to-tail stacked cyclodextrin pairs, and in consequence, only 2/3 of the crown ether units in 1/3 of the cyclodextrin layers interact with a cation, the others remaining "empty".

Since the salt-free structure[367] possesses an analogous spatial guest-host relationship, the cations cannot be solely responsible for the uniform conformation and orientation of the crown ether in the cavity. Most remarkably in all these structures is the close correspondence between hydrophilic and hydrophobic surface areas at the guest-host contact.

Some General Remarks on the Hydrophobic Guest-Host Relationship and the Molecular Recognition of Cyclodextrins

Albeit the MLP's of the inclusion complexes presented here strongly support the notion that the final relative orientation of the guest inside the host cavity is not only determined by dipole-dipole interactions, but also by the hydrophobic topographies of both reaction partners, no conclusions on the kinetics of the inclusion process could be drawn from these molecular modelings. The structures shown here represent equilibrated (solid state) geometries, which reflect the thermodynamic stability of the

product. It is therefore basically wrong, to deduce from the MLP's the direction from which the guest molecule enters the cavity of the cyclodextrin. On first sight it could be assumed that hydrophobic guest molecules enter the interior of the cyclodextrin through the hydrophobic 6-CH_2OH aperture, but as outlined above in detail, this side represents the narrow opened end only. From the steric point of view, it becomes more reasonable that the ligand enters from the opposite wide-opened torus rim passing the hydrophilic 2,3-OH groups. This proposal was in particular confirmed by a molecular mechanics study of *p*-hydroxybenzoic acid entering α-CD and evaluation of the corresponding energy potential surface as a function of the depth of penetration and the relative orientation of both reactants (rotation of the guest). A relatively small energy barrier for the 2,3-OH entrance was confirmed, while on the opposite side a large barrier was found, which is not likely to be overcome at room temperature[325].

Obviously, the MLP's as well as the dipole-dipole interactions lock the guest molecule in its finally position once it has entered the cavity in the proper orientation (independent of the direction of entrance). Improper inclusion would lead to an expulsion of the ligand out of the cavity by the very same effects.

The chirality inherent in cyclodextrins enables them to differentiate between stereoisomeric potential guest molecules[422], or *vice versa*, to induce conformational enantiomerism of encapsulated achiral molecules. Albeit some direct hints for these effects can be obtained from solid state structural analysis[423], NMR data[424], and chromatographic separations using cyclodextrins as asymmetric stationary phases[425], the chiral resolution of the unmodified cyclodextrins is generally poor[319,360e,426].

It is the undirected nature of hydrophobic and van der Waals interactions which causes the significant lack of specificity during molecular recognition by the cyclodextrins. Even the distinct directionality of hydrogen bond interactions is opposed by the *pseudo n*-fold symmetry of the various cyclodextrins, which provides *n* alternative, but equally potent hydrogen bond donor and acceptor functions for stabilization of the molecular assembly. Chemically modified cyclodextrins[427] were considered as basic molecular models for enzymes[428-430] and transition state binding[431] (for a critical comment on this see the epilogue), but the observed regio- and stereospecificity, and thus, the differentiation between different substrates remains low. In the sequel it is outlined for one example of substituted cyclodextrins, how chemical modification can alter the physico-chemical properties of cyclodextrins in a very pronounced fashion.

Cyclodextrins with Inverse Hydrophobicity

In the above sections it was outlined that unsubstituted cyclodextrins exhibit a distinctive hydrophobic central cavity, while the outside is considerably more hydrophilic. Due to this general property, the natural cyclodextrins are also considered as "exohydrophilic" host molecules. Remarkably effort has been spend on the synthesis of chemically modified cyclodextrin derivatives[427]: per-*O*-alkyl substituted cyclodextrins – most notably the per-*O*-methylated derivatives – exhibit a significantly amphiphilic behavior. By crystallization from aqueous solutions inclusion complexes with hydrophobic organic compounds can be obtained. However, Menger *et al.*[432] found an entirely different behavior for heptakis(3-*O*-butyl-2,6-di-*O*-methyl)-β-cyclodextrin in organic solvents: in *n*-heptane solutions relatively polar guests like *p*-nitrophenol are easily incorporated in the cyclodextrin cavity, while more polar solvents weaken the corresponding binding constants in a very pronounced fashion.

In the sequel, it is tried to comprehend the finding of opposite solvent effects on the complex stabilities of unsubstituted and *O*-alkylated cyclodextrins by means of their MLP's. The availability of solid state structural data of many hexakis(2,3,6-tri-*O*-methyl)-α-cyclodextrin[433] and heptakis(2,3,6-tri-*O*-methyl)-β-cyclodextrin[322,434] inclusion complexes represents an excellent starting point for molecular modeling studies.

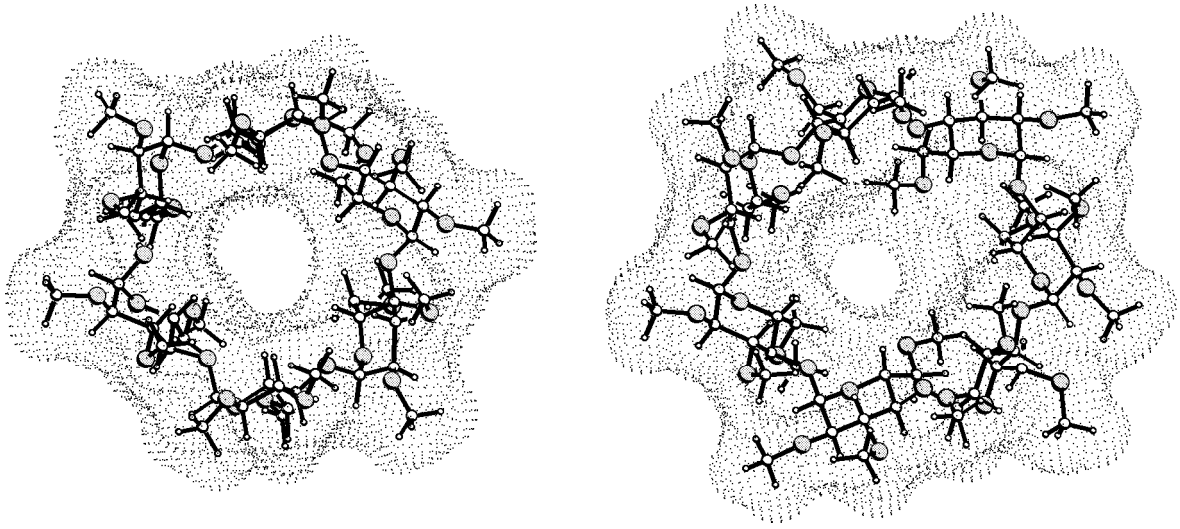

Fig. 6-20. Dotted contact surfaces of representative per-*O*-methyl α- (*left*) and β-CD units (*right*). The cyclodextrin structures were obtained from the solid state structures of the hexakis(2,3,6-tri-*O*-methyl)-α-cyclodextrin iodoacetic acid clathrate monohydrate[433e] and heptakis(2,3,6-tri-*O*-methyl)-β-cyclodextrin (*S*)-2-(2-fluoro-biphen-4-yl)propionic acid[434d] inclusion complexes after removal of the guest.

The per-*O*-methylated α- and β-CD units extracted from the crystal structures of the iodoacetic acid clathrate monohydrate[433e] and (*S*)-2-(2-fluorobiphen-4-yl)propionic acid[434d] inclusion complexes were chosen as representative examples for not highly tensed structures – their contact surfaces are shown in Fig. 6-20 in the common dotted form. Due to steric hindrance between the methyl groups and the lack of a stabilizing hydrogen bond network at both the torus rims, the macrocyclic ring of the methylated cyclodextrins is generally more flexible and more pronouncedly distorted than the OH-free cyclodextrins are[319,434b]. Detailed ^{1}H- and ^{13}C-NMR studies indicated that the steric effects introduced by *O*-methylation lead to flattened-shape geometries of the macrocycle in solution[435], which are in good agreement with X-ray structural data. The per-*O*-methyl α- and β-CD shown in Fig. 6-20 exhibit wide ranges of glucose tilt angles (α-CD: $\tau \approx 91 - 106°$ and $<\tau> \approx 106(10)°$; β-CD: $\tau \approx 77 - 128°$ and $<\tau> \approx 108(20)°$) and asymmetrically distributed O_1-$O_{1^{n'}}$-distances that reflect elliptical distortions (α-CD: 8.24 – 8.72 Å, $<d(O_1\text{-}O_{1^{n'}})> \approx 8.5(3)$ Å), and $d_{min}/d_{max} \approx 0.94$; β-CD: 9.26 – 10.15 Å, $<d(O_1\text{-}O_{1^{n'}})> \approx 9.7(4)$ Å), and $d_{min}/d_{max} \approx 0.91$). The macrocycle of the α-CD unit is less puckered ($<|\theta_{O\text{-}O}|> \approx 7.0(4.0)°$ and $<d_{O1}> \approx 0.14(5)$ Å) than the one of the larger β-CD ($<|\theta_{O\text{-}O}|> \approx 15(8)°$ and $<d_{O1}> \approx 0.36(18)$ Å). The cross section plots (cf. Fig. 6-7) through the corresponding Connolly surfaces (Fig. 6-21, compare to Fig. 6-8) indicate a slightly increased torus diameter when compared with the unsubstituted parent compounds. In both cases, the cavity is narrowed to some extent in the middle, but widened at the 2,3-OH aperture.

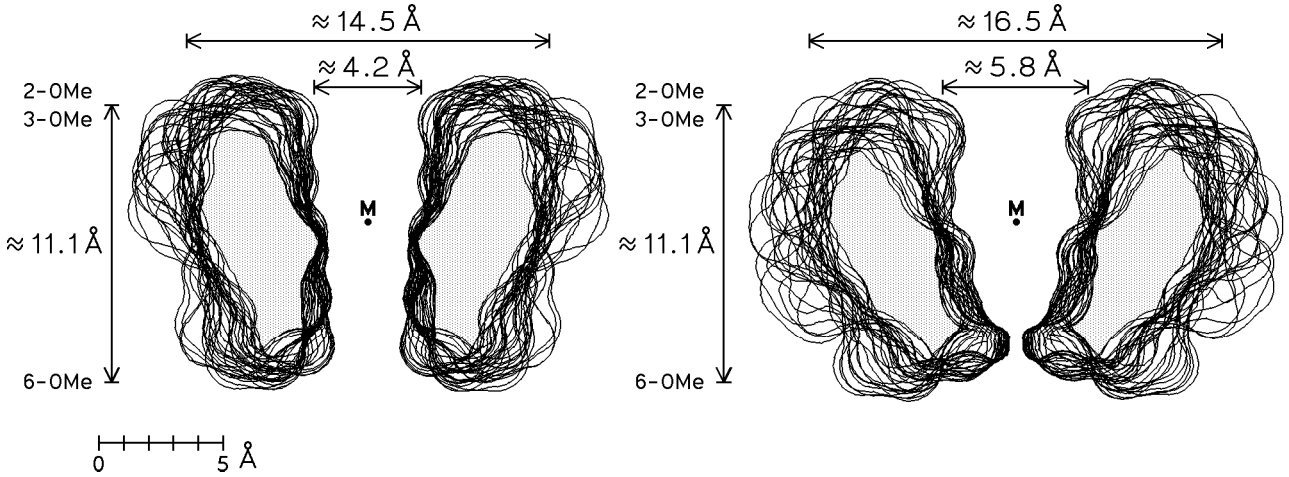

Fig. 6-21. Cross section plots (cf. Fig. 6-7) through the contact surfaces of the permethylated α- (*left*)[433e] and β-CD units (*right*)[434d] derived from solid state structures of inclusion complexes (cf. Fig. 6-20). As in Fig. 6-8, the approx. molecular dimensions are indicated (*M*: center of geometry).

Due to the pronounced extension in height (≈ 11.1 Å as related to ≈ 8.1 Å for α- and β-CD) the volume of the cavity is increased by approximately 10 – 20 % (per-*O*-methyl α-CD: 120 and β-CD: 180 Å^3, versus calculated total apparent molar volumes $^{\phi}V$ of 1400 and 1645 Å^3, respectively).

Following the methodology outlined above, the MLP's calculated on the Connolly surfaces of both the per-*O*-methyl α- and β-CD derivatives are visualized in Fig. 6-22 by using the same color-code as applied previously. From these pictures, remarkably differences between the cyclodextrins and their derivatives become evident: the front- / back-side separation of hydrophilic and hydrophobic surface regions, which is primarily caused by the spatial relationship of the primary and secondary hydroxyl groups on opposite torus apertures of the natural cyclodextrins, is almost completely surpressed by *O*-methylation. Since both sides are covered by an equally dense layer of methyl groups they are almost similar in hydrophobicity. Even more elucidative are the side view models in Fig. 6-22: a central and less hydrophobic surface band is wrapping around the cyclodextrin torsi. In particular from the clipped surface models, it becomes evident that the least hydrophobic, i.e. the most hydrophilic surface areas are located on the inner sides of the cavities.

Compared with the total surface areas of approximately 970 (per-*O*-methyl α-CD) and 1130 Å^2 (per-*O*-methyl β-CD) the cavities comprise only estimated regions of 120 and 180 Å^2, respectively. But obviously, their inverted type of the hydrophobicity profiles implies far-reaching consequences on the physico-chemical properties of these compounds. As noted by Menger *et al.*[432], an essential prerequisite for the formation of cyclodextrin inclusion complexes are the differences in polarity (i.e. hydrophobicity) between the cavity of the host and the solvent. In aqueous solutions hydrophobic guest molecules are attracted by the apolar "polyether-like" interior of the cyclodextrin cavity. On the opposite side, in organic solvent-systems these ether-type oxygens lend to the – limited, but nevertheless clearly obvious – hydrophilic character of the central cavity as compared to the cyclodextrin outside surface area. Now in turn, the cavity is amenable to non-covalent binding of more polar substrates. Since no binding of *p*-nitrophenol to *O*-alkylated β-CD is observable in acetonitrile, it was concluded that the polarity of this solvent is sufficiently close to the hydrophobicity of the modified cyclodextrin cavity to mimic it efficiently and to prevent the guest molecule from encapsulation[432]. Along with hydrophobic interactions, intermolecular hydrogen bonding was proposed to contribute to the inclusion of *p*-nitrophenol[432].

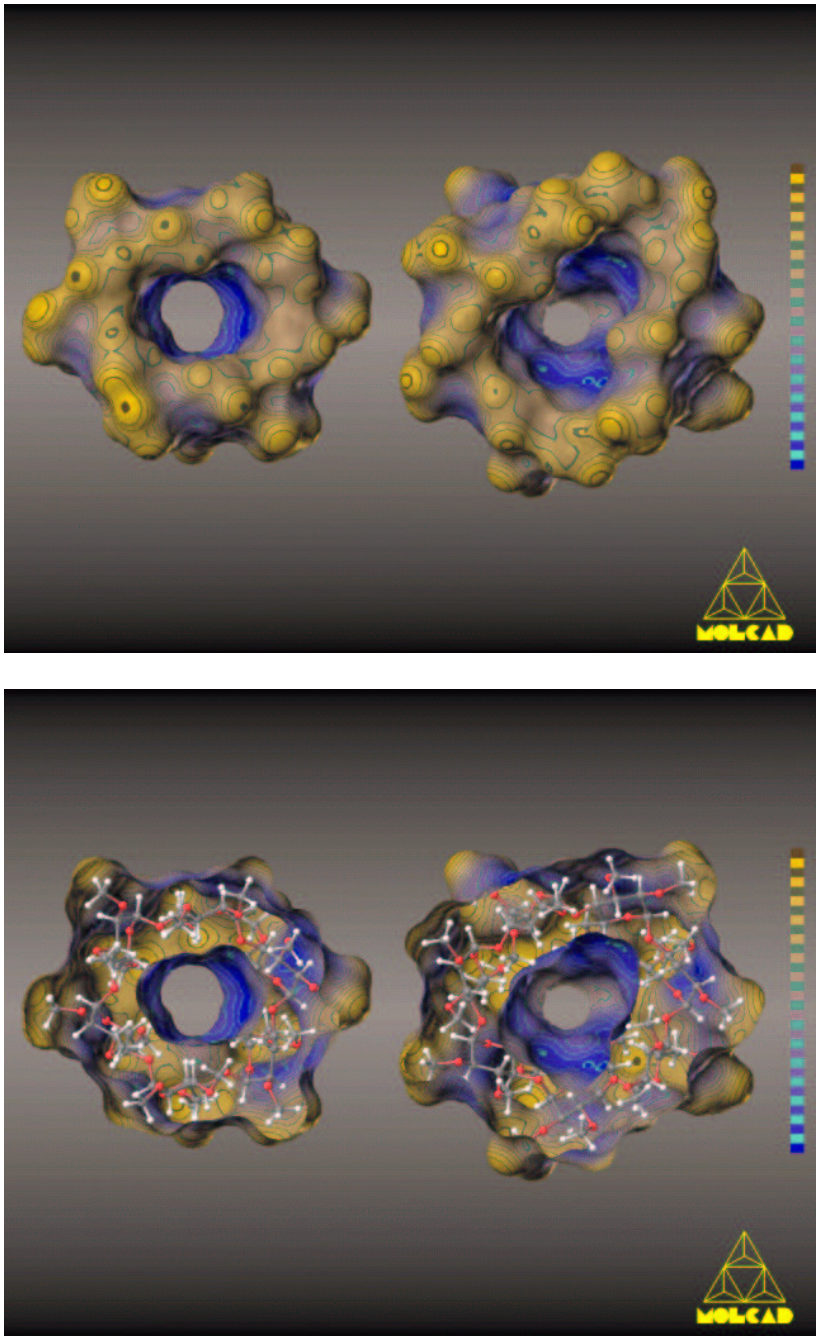

Fig. 6-22. Lipophilicity maps (color-code and molecular orientation cf. Fig. 6-9 on p. 162-163) for the guest-free cyclodextrin units of per-*O*-methyl α- (*left*)[433e] and β-CD (*right* each)[434d] (cf. Fig. 6-20). On the *left*, the 2-OMe / 3-OMe side of the cyclodextrins is displayed (cf. Fig. 6-6), the front half of the surfaces was removed in the *bottom* entry. The side view models (*top* entry) are aligned such that the 2-OMe / 3-OMe groups (larger opening of the tori) point upward, and the 6-CH_2OMe side (smaller aperture) faces downward. In particular the half-opened side views illustrate the hydrophilic (blue) character of the central cavities in relation to the hydrophobic (yellow-brown) outer surfaces. Since the applied color-code was adapted to the calculated range of MLP values for each molecule separately, it should be noted that no direct comparisons of the models presented here with those of Fig. 6-9 (unsubstituted cyclodextrins) should be made. *In toto*, the per-*O*-methyl cyclodextrins are much more hydrophobic than the parent compounds are, no absolute assignments are implied.

In consequence, the altered steric features and hydrophobic conditions inside the central cavities of the per-*O*-methyl cyclodextrins as compared with their natural precursors must lead to altered geometries of the inclusion complexes, too. Solid state structures indeed revealed distinct differences in the orientation and / or disposition of guest molecules within the cavity[319,433b,434b]. In particular the inclusion complexes of OH-free and methylated α-CD with benzaldehyde[406,433f] (*vide supra*) and *p*-nitrophenol[360c,433b] differ by opposite alignments of the guest in the cavity, which may be attributed to the opposing orientations of the MLP's ("inverse" hydrophobicity / hydrophilicity relationships). On the other hand, for *p*-iodoaniline[360a,404,433a] only different dispositions along the cyclodextrin axis were manifested.

The chiral resolution of unsubstituted cyclodextrins is rather low[319,360e], while the increased asymmetric distortion of the cavities seems to yield in an enhanced ability of the per-*O*-alkylated cyclodextrins to discriminate between enantiomeric guests[319,426,436]. Beside specific hydrogen bonding effects, the chiral recognition and the selective inclusion of one enantiomer out of a racemic mixture was proved to be mediated by "induced-fit" type changes of macrocyclic ring conformations. In addition, spatial fitting of apolar regions of the glucose residues towards hydrophobic moieties of the guest contributes thereto[319,433d,g,434c,d].

The still recurring wrong proposal of hydrophobic interactions to be not important for the formation of inclusion complexes in a very recent study on the binding characteristics of 8-anilino-1-naphthalenesulfonate towards per-*O*-methyl β-CD[437], can be attributed to an over-interpretation of the signs of enthalpy and entropy, and to a deficient knowledge of recent literature.

The natural cyclodextrins exhibit "poly-alcohol" type cavities that are able to accommodate even inorganic anions[379]. On the other hand, the "poly-ether" type interior of the *O*-alkylated derivatives resembles more closely a crown-ether in terms of the functional groups being present, and thus is able to act as complexing agents for cations. Upon suitable exchange of some *O*-alkyl groups versus *O*-acyl-groups – which support the incorporation of cations by providing additional potential binding groups – very strong hosts for metal ions in organic solvent are obtained[438]. In activity, but not selectivity, they even surpass the crown-ethers[308]. In summary, the substituted cyclodextrins exhibit inverted "exolipophilic"[308] characteristics, which to a large extent determine the properties of their inclusion complexes.

Epilogue

Albeit the fact, that on the first sight the choice of the cyclodextrin structures used within this study may seem somehow arbitrary, the selection was made in order to gain a representative survey of characteristic features within this class of compounds. This in particular holds true when remembering that computational studies vindicated the cyclodextrin hydrates to represent "frozen molecular images" of their solution states. Taking all the facts together, the molecular lipophilicity patterns (MLP) reveal rather uniform hydrophobic topographies for all cyclodextrins that are almost independent of their different ring sizes. Fine changes in the conformations of the cyclodextrins such as moderate variations in the glucose tilt angles and / or rotations of the hydroxymethyl groups do not alter the MLP's to a significant extent or change their basic implications. However, chemical modification via *O*-alkylation of the hydroxyl groups can alter the physico-chemical properties of the cyclodextrins substantially.

The multitude of structures presented here provides further corroborations for the pivotal importance of hydrophobic interactions for the formation of the inclusion complexes. It also should be noted that other types of interactions are important, too. Only in combination with polarization effects, dipole-dipole attractions, and van der Waals interactions, the remarkably high stability of many of these complexes becomes understandable. Enthaplic and entropic thermodynamic parameters compensate each other at least partially, and the relative contribution of each of the basic types of interactions to the total free energy of binding certainly varies as a function of the chemical nature of the guest. Thus, no attempts should be made to propose a single gradation of universal validity on the relevance of the various effects. The "induced-fit" mechanism that was suggested for α-CD, but not for β- and γ-CD (*vide supra*) is only one example in proof of this statement.

Particular in view of the still prevailing and rather controversial debate[307] about the "induced-fit"-type mechanism of the inclusion process, it is noteworthy that in a strict sense it must apply to all cyclodextrin complexes. It could hardly be imagined that the conformational properties of the cyclodextrin are not altered upon encapsulation of any guest, and that the cyclodextrin does not adapt to at least some extent its shape towards the altered conditions inside the cavity. It is thus not only misleading to deny the "induced-fit" for any of these complex structures, it is basically wrong. Only the relative importance of this process as compared with other interaction energies may alter from case to case. Experimental studies suffer from the currently prevailing dilemma that all types of interactions are almost inseparable interconnected with each other, and thus, an exact and unequivocal factorization of the Gibbs energy into various energy and entropy terms could no be made by experimental methods. It

may well be that only computational strategies provide tools sophisticated enough to study molecular systems on such a basic molecular level, which allows for the observation of experimentally inaccessible features of the system that can contribute to its more detailed understanding.

Referring to the common trend of considering chemically modified cyclodextrins[427] as basic models for enzymes[428], it must be noted that beside the rate enhancing effect on a particular chemical reaction almost no similarities between enzymes and cyclodextrins can be found. Not only the entirely different chemical structures (proteins *versus* carbohydrates) of both classes of compounds, but also their strikingly different mechanisms of molecular recognition must seriously call this concept into question. A large variety of different chemical groupings enables enzymes to specifically recognize their substrates via strong interactions of distinct directionality, which can be highly sensitive to even minor changes of stereochemical features of the ligand. The chiral cyclodextrins are also able to discriminate between enantiomeric guests or induce conformational enantiomerism upon inclusion, but the molecular interactions are generally weak and obviously lack any directionality. In addition to the C_n-symmetry axis of the "empty" cyclodextrin cavities, the absence of structural features that create strong guest-orienting forces indicates that the cyclodextrins can reach by no means the specificity and effectivity of the enzymes. In consequence, they should be seen more likely as simple template-effect based catalysts, which exert their effect on the reaction kinetics via bringing the substrate and the reagent into a close spatial relationship. The terminology of considering cyclodextrins as "enzyme models" only leads to an unjustified devaluation of nature's sophisticated tools. Relating the rather unspecific interactions between γ-CD and C_{60} with specific biological functions of C_{60}[370] seems to be fairly far-fetched.

In this chapter it was demonstrated how molecular modeling techniques can contribute to a straightforward assessment of the pivotal binding forces involved in the formation and self-assembly of the cyclodextrin inclusion complexes. In the following chapters it will be outlined, how to select out of the infinite number of cyclodextrin isomers and derivatives – which are (at least in principle) accessible via chemical synthesis – the most relevant and interesting ones. In view of the enormous man-power and time being invested nowadays in the synthesis of structures of growing complexity in such a fashionable field like supra-molecular chemistry[439], it deems appropriate to stand back a little and to think about the chemical principles of molecular association. Going back to the roots and rationalizing more exactly the origins of molecular recognition and the corresponding fundamental thermodynamic

principles would certainly be helpful in selecting more carefully what structures would be worth the immense effort of their synthesis. One would claim that it is still unclear how to design molecules with exactly pre-determined properties and that many centennial discoveries had been made by pure chance, but in view of the astronomically growing costs of basic research, computational methodologies should be applied to make proper pre-selections to save time and money. In also should be noted that computational strategies have to be planed very carefully, since (albeit the fact, that the major advantages and disappointments of many theoretical approaches are quite well known) many studies undertaken suffer from an unjustified oversimplification of the applied models and the basically wrong conclusions drawn therefrom. The non-availability of computational power is getting a less and less applicable argument to justify too simple techniques.

Appendix – Computational Methods

I. Molecular Structures. All cyclodextrin geometries were obtained from the Cambridge Crystallographic database, recent structure determinations were included as long as the atomic coordinates had been provided. Hydrogen atoms not included in the molecular structures were positioned geometrically with standard bond lengths $r_{C\text{-}H} \approx 1.08\,\text{Å}$ and $r_{O\text{-}H} \approx 0.90\,\text{Å}$, taking special care of intramolecular hydrogen bonding between neighbored hydroxyl groups. All given molecular parameters discussed within this study had been recalculated from this data set.

II. Geometry of δ-Cyclodextrin. From rigid body rotation and least-squares fitting[128] of the glucose residues of all α-, β-, and γ-cyclodextrins two mean glucose units (C_6O_6) with orientations of the hydroxymethyl grouping[66] either *gg* or *gt* were obtained. The atomic coordinates of δ-CD units were generated by rotation of these standard glucose units and least-squares fitting of their projections to each of the α-D-glucose moieties in the δ-CD plot in Ref. [320]. Subsequent assembly of all reoriented residues by fitting the O_1-atoms together yielded the overall conformation of the macromolecule with mean uncertainties in the coordinates of the O_1-atoms of $\approx 0.03\,\text{Å}$, hydrogen atoms were placed geometrically as described above.

III. Molecular Surfaces and Hydrophobicity Patterns. Calculation of the molecular contact surfaces and the hydrophobicity patterns was performed with the MOLCAD molecular modeling program, the computational basics are given by Brickmann *et al.* in Ref. [58] and in Chapter 3. Surface coloring was achieved using texture mapping techniques[59], graphics were photographed from the computer screen of a SILICON-GRAPHICS workstation.